Master Thesis

Czech Technical University in Prague

F3

Faculty of Electrical Engineering
Department of Telecommunication Engineering

Coexistence of optical systems on a physical layer

Bc. Milan Chvalina

Supervisor: Ing. Michal Lucki, Ph.D.
Field of study: Electronics and Communication
Subfield: Photonics
May 2021

ZADÁNÍ DIPLOMOVÉ PRÁCE

ČVUT
ČESKÉ VYSOKÉ UČENÍ TECHNICKÉ V PRAZE

I. OSOBNÍ A STUDIJNÍ ÚDAJE

Příjmení: **Chvalina** Jméno: **Milan** Osobní číslo: **465954**

Fakulta/ústav: **Fakulta elektrotechnická**

Zadávající katedra/ústav: **Katedra elektromagnetického pole**

Studijní program: **Elektronika a komunikace**

Specializace: **Fotonika**

II. ÚDAJE K DIPLOMOVÉ PRÁCI

Název diplomové práce:

Koexistence optických systémů na fyzické vrstvě

Název diplomové práce anglicky:

Coexistence of optical systems on a physical layer

Pokyny pro vypracování:

Cílem práce je studium možností současného provozování více optických systémů na společné fyzické vrstvě za různých podmínek zatížení sítě. Dílčím cílem je porovnání integrace systémů o různých rychlostech, různé kanálové rozteči nebo používajících odlišné modulace či výkonové úrovně; CWDM, DWDM, PON, AON a další. Soustřeďte se na republikové sítě s dosahem přibližně 400 km. Simulace provádějte v prostředí Optsim a s ohledem na doporučení ITU-T v této oblasti. Finálním výsledkem jsou modely koexistence různých přenosových systémů a prostředků a teoretické úvahy o tom, které systémy a za jakých podmínek lze pomyslně slučovat a u kterých systémů či variant nasazení se tento postup nedoporučuje.

Seznam doporučené literatury:

[1] ITU-T G-series Supplement 39: Transmission systems and media, digital systems and networks. ITU, 2012.
[2] CHANDRASEKHAR S., LIU X., FAUCONNIER T, CHARLET G. a BIGO S., Impact of Channel Plan and Dispersion Map on Hybrid DWDM Transmission of 42.7-Gb/s DQPSK and 10.7-Gb/s OOK on 50-GHz Grid. IEEE Photonics Technology Letters. IEEE, 2007.
[3] UDALCOVS, A., P. MONTI, V. BOBROVS, R. SCHATZ, L. WOSINSKA a G. IVANOVS. Spectral and energy efficiency considerations in mixed-line rate WDM networks with signal quality guarantee. 2013 15th International Conference on Transparent Optical Networks (ICTON). IEEE, 2013

Jméno a pracoviště vedoucí(ho) diplomové práce:

Ing. Michal Lucki, Ph.D., katedra telekomunikační techniky FEL

Jméno a pracoviště druhé(ho) vedoucí(ho) nebo konzultanta(ky) diplomové práce:

Datum zadání diplomové práce: **12.02.2021** Termín odevzdání diplomové práce: ________

Platnost zadání diplomové práce: **30.09.2022**

[redacted]	[redacted]	[redacted]
Ing. Michal Lucki, Ph.D. podpis vedoucí(ho) práce	podpis vedoucí(ho) ústavu/katedry	prof. Mgr. Petr Páta, Ph.D. podpis děkana(ky)

III. PŘEVZETÍ ZADÁNÍ

Diplomant bere na vědomí, že je povinen vypracovat diplomovou práci samostatně, bez cizí pomoci, s výjimkou poskytnutých konzultací. Seznam použité literatury, jiných pramenů a jmen konzultantů je třeba uvést v diplomové práci.

29.4.2021	[redacted]
Datum převzetí zadání	Podpis studenta

Acknowledgements

I would like to thank my family and friends for their continuous support and love throughout my studies. Special thanks go to my supervisor Ing. Michal Lucki, Ph.D. for his guidance, patience and invaluable advice when writing this thesis

Declaration

I declare that the presented work was developed independently and that I have listed all sources of information used within it in accordance with the methodical instructions for observing the ethical principles in the preparation of university theses.

Prague, May 1, 2021

Prohlašuji, že jsem předloženou práci vypracoval samostatně a že jsem uvedl veškeré použité informační zdroje v souladu s Metodickým pokynem o dodržování etických principů při přípravě vysokoškolských závěrečných prací.

V Praze, 1. května 2021

Abstract

This thesis deals with coexistence of optical systems on a physical layer. The main objective of this thesis is to analyse interactions between multiple optical systems at the physical layer, while partial goal is to compare the integration of these systems under different system conditions. Data for this study were obtained by computer simulation in Optsim environment. On the basis of the resulting models of coexistence of different transmission systems under various system conditions it can be concluded, whether it is recommended to combine certain systems or not.

Keywords: DWDM, Fibre Optic Communications, Physical Layer, Optsim, Coexistence

Supervisor: Ing. Michal Lucki, Ph.D.
Fakulta elektrotechnická,
Technická 1902/2,
166 27 Praha 6

Abstrakt

Tato diplomová práce se zabývá koexistencí optických systémů na společné fyzické vrstvě. Cílem této práce je analýza interakcí mezi různými optickými systémy na fyzické vrstvě, přičemž dílčím cílem je porovnání integrace těchto systémů za různých provozních podmínek. Data pro tuto práci byla získána pomocí simulačního prostředí Optsim. Na základě výsledků koexistence různých systémů za různých provozních podmínek lze vyvodit závěr, zda je možné systémy sloučit či se tato varianta nasazení nedoporučuje.

Klíčová slova: DWDM, Komunikace pomocí optických vláken, Fyzická vrstva, Optsim, Koexistence

Překlad názvu: Koexistence optických systémů na fyzické vrstvě

Contents

Figures

Tables

Chapter 1
Introduction

1.1 General Background

It is possible to observe ever increasing growth of bandwidth demands over the past few years. As we are now facing a challenge caused by global pandemic, the Internet connectivity has become even more important than ever before. Business meetings, lectures, friends calls and many other activities are done online. As the new applications keep on emerging, future telecommunication networks are expected to be increasingly heterogeneous with respect to applications supported and underlying technologies employed. Since a greenfield network design is an extremely expensive project, another solution has to be found. To address this heterogeneity, it may be most cost effective to set up different lightpaths at different bit rates in such a backbone telecommunication network employing optical wavelength division multiplexing. This approach can be cost effective because low-bit-rate services will need less multiplexing with other low bitrate services onto high capacity wavelengths, while a high bitrate service can be accommodated directly on a wavelength itself. Optical networks with Mixed Line Rates (MLRs), e.g., 10/40/100 Gbit/s over different wavelength channels, are therefore a new networking paradigm. However, drawbacks are also present [1] [2].

Although Mixed Line Rates networks are energy and cost efficient, number of issues have to be addressed. Transmission of high bit rates is surely desirable because it can carry a huge amount of traffic, but at such high bit rates, the Physical Layer Impairments (PLI), such as dynamic impairments (Self-Phase modulation, Cross-phase modulation, Four Wave Mixing) and static impairments (dispersion, optical amplifier noise, crosstalk, optical filter concatenation, laser frequency offset and receiver noise), significantly limit the reach of the regenerator-free optical distance. So, in the context of wavelength-division multiplexed (WDM) backbone telecommunication networks, increasing the capacity of a wavelength to 100 Gb/s presents a tradeoff between capacity and reach [2].

Channel spacing is also an important issue. Assuming fixed channel spacing, it is necessary to determine the optimum value of channel spacing. When the channel spacing is low, high-bit-rates channels get band-limited, and thus their bit error rate (BER). On the other hand, if the channel spacing is high, the low-bit-rates channel may have poor BER because of the optical noise [3].

Besides accommodating a continuously growing traffic that additionally results in even more heterogeneous nature of traffic demands, network providers have to deal with an overall network power consumption that increases due to extra signal regeneration required because of the even higher spectral efficiency. In [4], assessment of the trade-off between spectral efficiency and the power consumption in a WDM transport network, when a certain quality of transmission (BER= 10^{-9}) needs to be guaranteed at the receiving node, was made. It was found that 100 Gbps DP-QPSK channels guarantee good power efficiency performance (W/bps) as long as the needed capacity is larger than 80 Gbit/s and the end-to-end transmission distance does not exceed a certain threshold of fibre length. For longer transmission distances the cost of the optical signal regeneration becomes too high and Mixed Line Rate (MLR) design solutions using mainly 40 Gbps NRZ-DPSK channels become more appealing. Similar study was conducted in [5], where power consumption per transmitted bit per second (W/bps) for the number of 10/40/100 Gbit/s Mixed Line Rate and Single Line Rate (SLR) solutions have been compared for end-to-end connections of different lengths over Wavelength Division Multiplexing (WDM) networks with high spectral efficiency while guaranteeing an error probability for signal detection not higher than 10^{-9} at the receiving node. The results show that MLR design mostly outperforms SLR design. However, in some cases SLR could also be an appealing solution and cannot be considered out of contention.

1.2 Objectives

The main objectives of this thesis are as follows:

- Provide an overview of the theoretical framework for understanding and correct interpretation of phenomena, which occur in an optical system
- Describe methods used in this thesis for data collection and its interpretation
- Present models of coexistence of different transmission systems under various system conditions, while making recommendations on how to combine certain optical systems

1.3 Overview of The Structure

This thesis is structured into 4 chapters. Chapter 2 contains theoretical background and review of relevant literature. This chapter discusses general phenomena in optical systems providing basis for understanding of channel coexistence. The methods used in the study are then described in Chapter 3, after which the results are presented and discussed in Chapter 4. Finally, Chapter 5 outlines the main conclusions and identifies both limitations to the study and recommendations for further research.

Chapter 2

State of The Art

2.1 Wavelength Divison Multiplexing

Wavelength Division Multiplexing (WDM) is a fibre-optic transmission technique that enables high transmission capacity by transmitting several (hundreds) wavelengths over one fibre. WDM system consists of n transmitters and receivers. Each modulated signal is transmitted on its wavelength. All wavelengths are then multiplexed in a multiplexer and transmitted over a fibre. In order to make demultiplexing possible, wavelengths have to be orthogonal to each other and separable enough. Multiplexed channels are then demultiplexed in a demultiplexer and each signal is detected by respective receivers. Overall system capacity is then determined by the relation

$$B_T = B_1 + B_2 + \ldots + B_n, \tag{2.1}$$

where B_T is total bitrate and B_i is a bitrate of i^{th} channel [6].

As the development has continued over time and the number of wavelengths rose, the need for standardization and unification of usable bands, channel width, pilot wavelength and channel spacing has intensified. Nowadays, there is a standard called Coarse Wavelength Division Multiplex (CWDM) within the recommendation of ITU-T G.694.2 and Dense Wavelength Division Multiplex (DWDM) within the recommendation of ITU-T G.694.1. Both recommendations will be discussed in the next subsections [6].

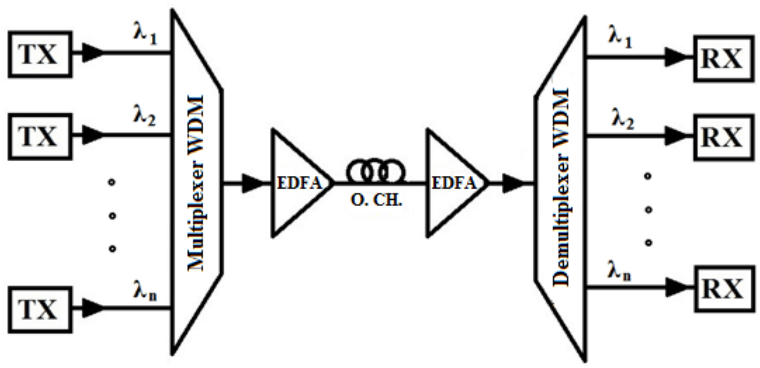

Figure 2.1: The principle scheme of WDM system, taken from: [7]

2.1.1 Coarse Wavelength Division Multiplexing

By CWDM standard is channel width relatively wide and channel spacing low, as the word „coarse" implies. Figure 2.2 and table 2.1 show CWDM wavelength grid and nominal central wavelengths.

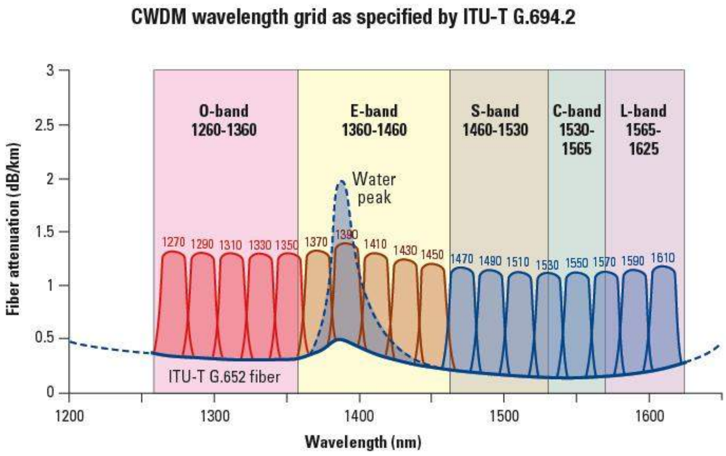

Figure 2.2: CWDM wavelength grid, taken from: [8]

Channel number	27	29	31	33	35	37
Central wavelength [nm]	1271	1291	1311	1331	1351	1371
Channel number	39	41	43	45	47	49
Central wavelength [nm]	1391	1411	1431	1451	1471	1491
Channel number	51	53	55	57	59	61
Central wavelength [nm]	1511	1531	1551	1571	1591	1611

Table 2.1: CWDM nominal central wavelengths, edited from ITU-T G.694.2

By CWDM standard the first channel is defined at 1271 nm and the last one at 1611 nm with channel spacing 20 nm and total source wavelength variation of the order of ± 6-7 nm. Therefore it is possible to apply cheaper optical sources with wide spectral characteristics. Wavelength of generated electromagnetic radiation is also less precise and the requirements for wavelength stability are not high either.

CWDM multiplexing is used predominantly at the level of metropolitan networks (MAN), where distances reach up to tens of kilometres. One of the major advantages of CWDM is ease of implementation. Relatively cheap, uncooled VCSEL lasers meet CWDM requirements and thanks to their lower consumption in comparison with DWDM lasers are also more economical. Since channel spacing is relatively high, expensive tunable filters with high precision are not necessary. A negative consequence of high channel spacing is, however, relatively low capacity of WDM system. It is possible to use only 18 channels in the whole wavelength band. In addition, the are relatively big differences between channels in terms of chromatic dispersion and attenuation.

While attenuation in O-band is around 0,35 dB/km, in C and L-band it is around 0,22 - 0,3 dB/km. As a result, significant differences in attenuation between wavelengths could occur. In practise, channels from S, C and L bands are therefore deployed for longer distances, whereas channels from O and E bands for local metropolitan networks [6].

2.1.2 Dense Wavelength Division Multiplexing

ITU-T G.694.1 recommendation specifies Dense Wavelength Division Multiplex. By this standard, far narrower channels with strict tolerance and low channel spacing are defined. Unlike CWDM standard, DWDM makes use of only 2 wavelength bands - C and L band [6]. Fig. 2.3 depicts an illustration of DWDM and CWDM bandwidth division.

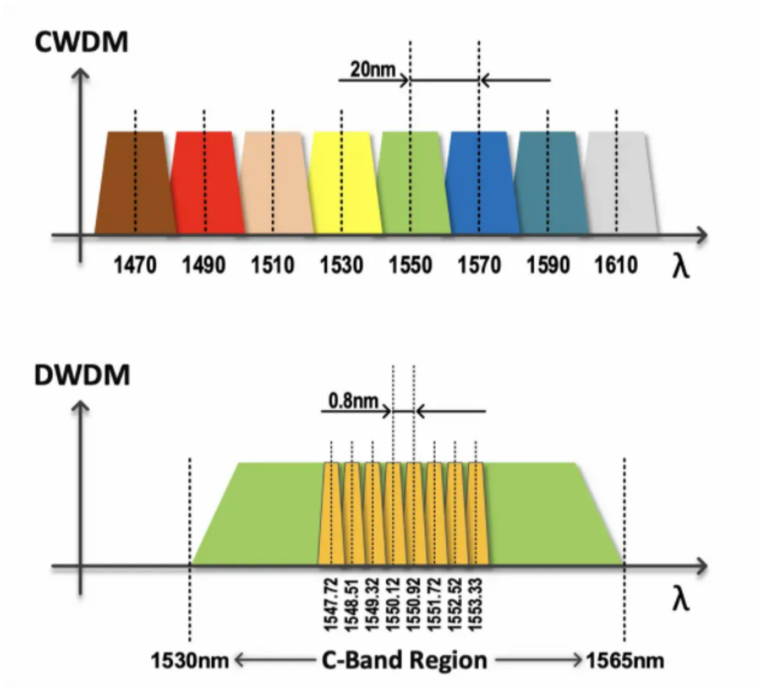

Figure 2.3: Illustration of DWDM and CWDM bandwidth division, taken from: [9]

Dense wavelength multiplexing defines 4 types of channel width:

- Channels with width 12,5 GHz (corresponds to the channel spacing of 0,1 nm). Carrier frequency is determined by the relation

$$193,1 + n \cdot 0,0125 \text{ [THz]}, n \in \langle -688; 227 \rangle \tag{2.2}$$

- Channels with width 25 GHz (corresponds to the channel spacing of 0,2 nm). Carrier frequency is determined by the relation

$$193,1 + n \cdot 0,025 \text{ [THz]}, n \in \langle -344; 113 \rangle \tag{2.3}$$

- Channels with width 50 GHz (corresponds to the channel spacing of 0,4 nm). Carrier frequency is determined by the relation

$$193,1 + n \cdot 0,05 \text{ [THz]}, n \in \langle -172; 56 \rangle \tag{2.4}$$

- Channels with width 100 GHz (corresponds to the channel spacing of 0,8 nm). Carrier frequency is determined by the relation

$$193,1 + n \cdot 0,1 \text{ [THz]}, n \in \langle -86; 28 \rangle \tag{2.5}$$

where n is an integer including zero. If $n = 0$, then the frequency is called pilot frequency and equals 193,1 THz (corresponds to 1552,5244 nm, speed of light c equals to $2,99792458 \cdot 10^8$ m/s according to ITU-T G.694.1 recommendation). Another distinction between standard G.694.1 DWDM and G694.2 CWDM is so called flexible DWDM channel. It is possible to create besides fixed channels also flexible channels with variable width defined in certain slots and combine them, unless they overlap. Carrier frequency of flexible channel is determined by relation

$$193,1 + n \cdot 0,00625 \text{ [THz]}, n \in \langle -1376; 448 \rangle \tag{2.6}$$

whereas channel width is defined as

$$m \cdot 12,5 \text{ [THz]}, m \in (0; 912 \rangle \tag{2.7}$$

From previous equations it is evident that slot width is a multiple of 12,5 GHz and carrier frequency differs from pilot frequency in steps of 6,25 GHz [6]. Illustration of flexible and fixed channels is shown in fig. 2.4.

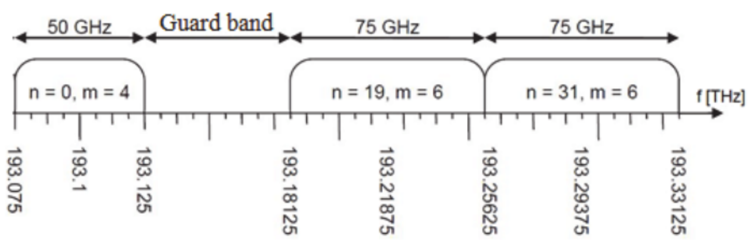

Figure 2.4: Illustration of fixed and flexible DWDM channels, taken from: [10]

Comparing CWDM and DWDM standard, there is an evident rise in usable channels. They are a lot narrower than CWDM channels and their number is therefore a lot higher. Furthermore, DWDM standard only uses C and L band, where attenuation dependence on wavelength is almost constant, which results in small differences in attenuation between channels. The main disadvantage is a requirement for temperature stabilization of lasers with narrow spectral characteristics. Not only are these laser expensive to purchase, but also to operate. As a result, DWDM is mainly deployed in backbone optical networks for transmission over large distances, where large transmission capacity is needed [6].

2.2 Dispersion in optical fibres

Dispersion in optical fibres is one of the most limiting factors in optical systems. In general, dispersion could be described as a pulse extension or compression (if dispersion is negative) in time domain while propagating through the fibre. If there is a digital stream of data, the pulses could be misinterpreted by the detector, because the extension of a pulse could overlap the logical state „0". This phenomenon is called Inter Symbol Interference (ISI). Since dispersion functions as a low pass filter, which limits the bandwidth, it needs to be compensated to achieve high bitrates [11].

2.2.1 Chromatic dispersion compensation techniques

Since most of the DWDM systems are operated in the C band, the chromatic dispersion of a standard Single Mode Fibre (SMF) has to be taken into account. There are 3 most widely used techniques to compensate chromatic dispersion:

- Dispersion Compensating Fibre (DCF)
- Fibre Bragg Grating (FBG)
- Electronic Dispersion Compensation (EDC)

In practice, the most common compensation technique for chromatic dispersion is probably Dispersion Compensating Fibre (DCF). This fibre has a high and mainly negative coefficient of chromatic dispersion. When DCF is connected with standard SMF, chromatic dispersion coefficients adds up and overall dispersion decreases almost to zero. Although this is a widely used technique due to its simplicity, it has its shortcomings. DCF is stored in a passive component called DC module (Dispersion Compensating Module). This module inserts insertion loss of 5 - 9 dB in the route. Furthermore, the core diameter is small, which could result in a generation of nonlinearities.

Fibre Bragg Gratings have emerged as major components for dispersion compensation because of their low loss, small footprint, and low optical nonlinearity. Fibre Bragg Grating functions as a filter, which reflects particular wavelengths and transmits others. This is achieved by a periodic variation in the refractive index of fibre core. The period is not constant and shortens along the propagation axis. This way are shorter wavelengths reflected deeper in the FBG grating than longer wavelengths.

A number of experiments have been conducted to find the most appropriate solution. In [12], the best results were obtained by using FBG in pre-compensation configuration comparing DCF and FBG in both pre- and post-compensation configurations. Examination of the long haul optical link up to 4000 km in the presence of using various modulation formats and dispersion compensation schemes was conducted in [13]. Symmetrical DCF compensation technique shows better performance in terms of Q value, BER and eye opening comparing pre, post and symmetrical schemes. It also enhances the transmission distance up to 4000 km with the acceptable value of Q. Furthermore, performance of OOK, DPSK and Duo-binary modulation scheme at 40 Gbps under no, pre, post, symmetrical and modified symmetrical dispersion compensation scheme using DCF was discussed in [14]. The modified symmetrical compensation technique turned out to be superior to other compensation techniques, when the first part of dispersion compensating fibre is placed in between optical combiner and the single mode fibre, the second part in midway of the SMF and the third part in between and, single mode fibre and optical splitter.

2.2.2 Polarization mode dispersion compensation techniques

Unfortunately, even if chromatic dispersion is compensated, other dispersion phenomenona occur, namely Polarization Mode Dispersion (PMD). Electromagnetic field of any mode could be divided into 2 orthogonal modes, where vectors E and H are perpendicular to each other. In practice, every fibre has some tiny geometrical imperfections that bring about inner tension. This results in anisotropic environment, where index of refraction depends on direction. Although PMD is usually small, it could have detrimental effect on data transmission over long distances at very high data rates, because portions of the transmitted signals in different polarization modes will arrive at slightly different times. This will again lead to increased BER. Moreover, PMD is a process, which is difficult to compensate [11]. Illustration of PMD depicts fig. 2.5.

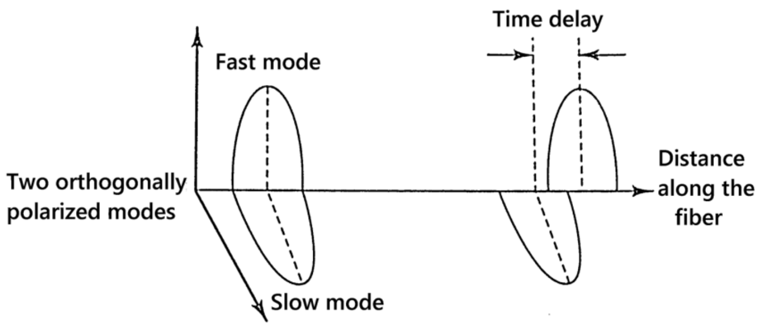

Figure 2.5: Illustration of polarization mode dispersion, taken from: [15]

All current methods applied for compensating PMD are extremely expensive and often not sufficiently effective. Basically, these compensation methods can be divided into optical, optoelectronic and electronic [16].

Optical compensation makes use of optical fibre with constant polarization (PMF) and polarization controller. Polarization maintaining fibres with high birefringence can maintain polarization state, as a result the level of differential group delay is set, which enables to compensate polarization mode dispersion. Such a fibre for residual dispersion compensation and PMD compensation is proposed in [17].

Optoelectronic method, on the other hand, is based on splitting up of the optical signal into fast and slow polarization components. Separated signals are converted to electric domain and one is appropriately delayed to minimise the differential group delay. Signals are then converted to the optical domain and combined. Such a method is proposed in [18], where effective PMD compensation was achieved using filter to inhibit noise impulses.

Electronic compensation of PMD in single-mode optical fibres is carried out by balancing the received optical signal, which is converted to an electric signal. The electronic compensation can be implemented by a transversal filter, a non-linear decision-feedback equalizer, different phase detection, etc. In [19], electronic equalization using digital filters is proposed, where pre-distortion and post-equalization methods are recommended.

2.3 Non-linear effects in optical fibre

Non-linear effects are other undesirable phenomena that must be taken into account in optical communications, although they can be useful in some applications. They could be divided into 2 categories: scattering effects and Kerr effects. In terms of scattering effects, there are 2 types of nonlinear scattering effects - Stimulated Brillouin Scattering (SBS) and Stimulated Raman Scattering (SRS).

SBS causes backward scattered light at a slightly lower frequency than the frequency of propagating wave. SBS may affect the performance of the transmission system in several ways. Firstly, the SBS threshold limits the input power, which results in maximally achievable SNR and transmission distance without gain. Secondly, re-directed Stokes wave can destabilize the transmitter, if the optical isolator is not properly inserted [20].

Stimulated Raman scattering, conversely, brings about the optical signal offset towards longer wavelengths. As a result, low frequency components are amplified, whereas high frequency components are attenuated. It has to be noted that power threshold for SRS is around 500 mW. Therefore SRS is not a problem for single-channel systems. However, in case of multi-channel system and optical waves matching the Stokes gain band, exchange of energy between the channels takes place. This presents a problem for DWDM systems, where power equality among channels is required [21]. Possible reduction method of SRS using Gaussian filter is proposed in [22].

Kerr effect, i.e., dependence of index of refraction on electric field, results in phenomena, which are detrimental to the optical systems, namely Self-Phase Modulation (SPM), Cross-Phase Modulation (XPM) and Four Wave Mixing (FWM).

Self-Phase Modulation occurs when the single optical pulse propagates through the fibre. Due to the refractive index dependence on power, the leading edge of pulse cause increase in refractive index, whereas its trailing edge cause decrease in refractive index. The leading edge of pulse shifts toward longer wavelength and trailing edge toward shorter wavelength causing frequency chirp of the transmitted signal.

In DWDM, there are multiple overlapping pulses resulting in Cross-Phase Modulation. The effect of XPM highly depends on the input power and number of channels. In [23], the impact of XPM on DWDM system and its compensation is discussed. Leaving some residual dispersion and increasing channels spacing led to increase of BER and Q-factor. XPM also degrades the systems performance of EDFA. Rigorous analysis was carried out in [24], where the effect of XPM on DWDM system was explained. Decrease in gain due to XPM was observed, however, varying parameters, such as EDFA length, pump power and signal power leads to a balanced configuration with better efficiency.

Four-Wave mixing (FWM) is a nonlinear optical phenomenon that generates new optical signals. If three optical signals with different carrier frequencies co-propagate inside a single optical fibre simultaneously, new frequency components could be generated at the expense of power depletion of the original channels. These mixing products can fall directly on signal channels resulting in crosstalks, as fig. 2.6 shows. New frequency components are generated according to the following equation

$$f_{ijk} = f_i + f_j + f_k, \tag{2.8}$$

where f_{ijk} are new frequency components and $f_{i,j,k}$ are original frequency components.

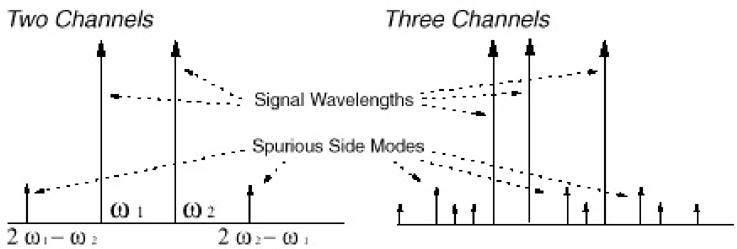

Figure 2.6: Illustration of Four Wave Mixing, taken from: [25]

As FWM induces signal degradation and additional noise, number of methods to minimize this effect has been proposed. In [26], variable channel spacing technique was described. In [27], thorough analysis of the channel crosstalk due to the FWM for various values of fibre length, core effective area, dispersion, channel spacing and channel power as a function of the number of multiplexed channels in a multi-channel system. The results show that the change of the crosstalk factor with the channel separation, fibre length, and core effective area are not significant compared to the variation in channel power and unequal channel spacing, while unrepeated unequal channel spacing performs better that repeated unequal channel spacing. Analysis of FWM based on varying system parameters is also explored in [28] and [29]. Another technique for FWM suppression was presented in [30], where circular polarizers were employed to set electric field of adjacent pulses at 180 degree of each other, resulting in lower FWM interaction of adjacent pulses. FWM reduction using optical phase conjugator (OPC) is introduced in [31], where the first OPC is placed in the midway of the fibre optic link and the other OPC is inserted after the second half of the fibre. This set up enables to remove FWM effect imposed on transmitted signal. Another solution for FWM was described in [32], where phase mismatch leading to FWM reduction was carried out by implementation of hybrid modulation technique, where trade off between low level of FWM products and reasonable Q-factor was achieved.

2.4 Erbium Doped Fibre Amplifier

Erbium Doped Fibre Amplifier (EDFA) plays a major role in modern DWDM systems. As signal propagates through the fibre over long distances, the signal gets attenuated and therefore has to be reamplified. Although EDFA has number of advantages, such as gain between 30-50 dB, amplification in C band and L band or independence on temperature and polarization, there are also some drawbacks, which has to be taken into account. One of them is dependence of gain on wavelength. EDFA has unflattened gain spectrum with a very sharp peak at around 1535 nm. As a result, different channels of DWDM system are amplified by different amounts. This is especially critical for long haul DWDM systems. Another problem is that like other amplifiers, EDFA is a main source of noise in the optical system, where the noise is caused by Amplified Spontaneous Emission (ASE).

There have been number of works dedicated to the optimization of EDFA parameters, such as pump power, length of the fibre or concentration of Erbium ions, in order to achieve low noise figure and flat gain for wide range of wavelengths. In [33] and [34], the system optimization by varying length of Erbium doped fibre or concentration of Erbium ions is outlined and optimal values based on simulation recommended. Similar studies are conducted in [35] and [36], where flattened gain for 16, respectively 32 channels, was achieved with noise figure around 7 dB and optimum values for pump power or length of Erbium doped fibre stated by means of simulation analysis. In [37], noise figure analysis was elaborated focusing on comparison between co-propagation at 980 nm EDFA configuration and counter propagation at 1480 nm configuration. Results show that in general, the pumping wavelength of 980 nm gives a stable noise factor values within 4 - 4.5 dB both for 10 m and 30 m long fibres. With the increase of pump power and fibre length, counter-propagation at pumping wavelength of 1480 nm provides noticeably higher noise up to 9-15 dB.

Investigation of EDFA positioning and its impact on the quality of the amplified signals was conducted in [38], where in-line configuration is recommended due to lower required pump power in comparison with booster configuration and more ASE noise comparing in-line and preamplifier configuration.

EDFA is also fundamental for ultra long-haul submarine networks. In [39], EDFA composed of three Erbium Doped Fibre stages assembled in a serial architecture with two Gain Flattening Filters (GFF) was presented. 70 nm of amplified bandwidth and output power level of 18.8 dBm was obtained by using only two pump lasers operating below 225 mW. The high output power and wide amplification bandwidth enables the transmission of up to 228 DWDM channels for more than 7000 km.

2.5 Modulations

A number of modulation formats are being examined as suitable candidates for the deployment in DWDM optical systems. They are compared in terms of their spectral efficiency, chromatic dispersion tolerance, optical reach or cost. This topic is thoroughly discussed in [40]. In this thesis 4 modulation formats with prospect of deployment in high speed optical networks were utilised. The goal was to analyse potential crosstalks or interactions between different optical systems sharing the same physical layer. NRZ-OOK modulation scheme serves as a reference, since most of the legacy WDM networks are based on this modulation format. Following subsections are dedicated to their description and implementation of transmitter and receiver in the following order

1. Non-return-to-Zero On/Off Keying (NRZ-OOK)
2. Differential Phase Shift Keying (DPSK)
3. Differential Quadrature Phase Shift Keying (DQPSK)
4. Polarization Multiplexed Quadrature Phase Shift Keying (PM-QPSK)

2.5.1 Non-return-to-Zero On/Off Keying

Non-return-to-Zero On/Off Keying (NRZ-OOK) is an intensity modulation format, which encodes information on the intensity of an optical signal. Logical state „1" corresponds to the certain power level of the laser source, whereas logical state „0" refers to the absence of an optical pulse. OOK can be implemented in RZ and NRZ format. Unlike RZ format, NRZ format permits constant optical intensity over several consecutive bits. RZ formats usually require a slightly more complex transmitter structure, but are generally more robust to Inter Symbol Interference (ISI) caused by imperfections in the frequency response and the limited bandwidth of optoelectronic transmitter and receiver hardware. In addition, RZ formats tend to be more robust to many nonlinear propagation distortions and PMD [41]. Nevertheless, the NRZ-OOK format was widely deployed due to its simple transmitter structure in legacy DWDM networks. However, due to increasing capacity demand, more advanced modulations format are needed. Such a capacity upgrade of existing 10 Gbit/s channels by 40 Gbit/s channels is described in [42] and [43], where interplay between neighbouring channels with different modulation format is studied.

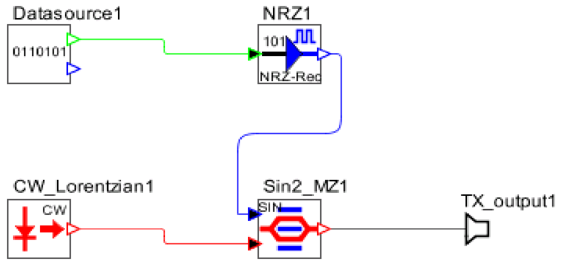

Figure 2.7: NRZ-OOK transmitter implementation

In Figure 2.7 transmitter implementation is depicted. Electronically generated NRZ waveforms are modulated by Mach-Zehnder Modulator (MZM) onto optical carrier, which is provided by laser operated in continuous wave regime. Receiver design for OOK modulation format is shown in figure 2.8. The receiver is made up of an optical band pass filter, which cuts out the respective channel from spectrum, PIN photodiode, which receives an optical power and converts it into electric current, and electrical low pass filter, which suppresses noise. Cut off frequency of such a filter, however, cannot be too low, because the spectrum of the received signal would be deformed and thus BER would increase.

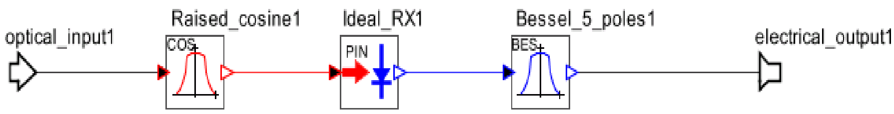

Figure 2.8: OOK receiver implementation

2.5.2 Differential Phase Shift Keying

DPSK is a phase modulation format, which encodes information on the binary phase change between adjacent bits. Logical 1 is encoded onto a π phase change, whereas logical 0 is represented by the absence of a phase change. Main advantage of using DPSK instead of OOK scheme is 3 dB sensitivity improvement, which results in better OSNR.

There have been number of experiments dedicated to the performance comparison of DPSK with OOK and other formats based on intensity modulation. It has to be noted that the modulation performance is dependent on a number of system parameters, including the dispersion compensation technique, bit rate, number of channels, channel spacing, receiver filter, and transmission impairments. Different conclusions may be drawn with different considerations [44]. In [45], performance analysis of various modulation formats (NRZ, RZ (33%, 50%, CSRZ 67%, CRZ), DB, RZ-DPSK, NRZ-DPSK) for access network based on WDM-PON and for different link distances and bit rates was performed. It was showed that DPSK performed significantly better for higher bitrates and longer distances. Nevertheless, for short distances and lower bitrates modulation formats such as CRZ or RZ achieved higher Q-factor. In [46], perfromance evaluation of different modulation formats (NRZ, RZ, CSRZ, DB, NRZ, NRZ DPSK, RZ-DPSK and CSRZ-DPSK) for 16-channel WDM passive optical network (WDM-PON) with transmission speed of 10 Gbit/s per channel was carried out. Among the investigated modulation formats, the best performance is yielded by DB and CSRZ-DPSK, when DB format allows to achieve longest transmission distance, However, CSRZ-DPSK showed more stable results in terms of BER while achieving comparable transmission distance.

Figure 2.9 shows NRZ-DPSK implementation. Phase of a signal from laser source is altered in a phase modulator according to the data stream. To perform optical phase modulation, one can either use a phase modulator PM or a Mach-Zehnder Modulator (MZM). Since exact phase modulation is more important for DPSK than a constant optical intensity, practical DPSK transmitters are most conveniently implemented using an MZM as a phase modulator [41].

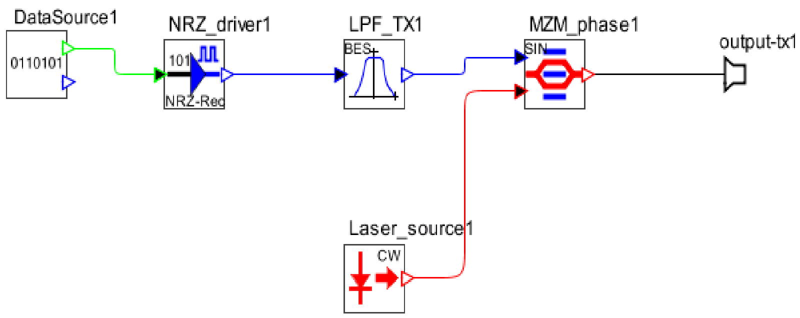

Figure 2.9: NRZ-DPSK transmitter implementation

Implementation of DPSK receiver is depicted in Figure 2.10. DPSK receiver is based on an optical band pass filter for channel selection, balanced DPSK receiver and electrical low pass filter for noise suppression.

Balanced DPSK receiver is composed of the tunable Mach-Zehnder interferometer having 2 optical output ports. In the interferometer, optical paths differ by a delay τ that must be set equal to the bit time duration. Each optical output is detected by an ideal PIN photodetector, and the output electrical signal is the difference between the detected currents [65].

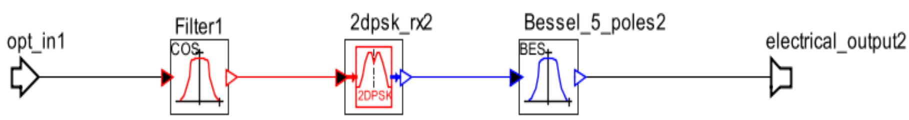

Figure 2.10: DPSK receiver implementation

2.5.3 Differential Quadrature Phase Shift Keying

Differential Quadrature Phase Shift Keying (DQPSK) is a multilevel modulation format, which transmits 2 bits of information in each symbol corresponding to the phase shift. It transmits four phase shifts $\{0, +\pi/2, -\pi/2, \pi\}$ at a symbol rate of half the aggregate bitrate. This is highly beneficial, because it either enables to double bitrate while keeping the symbol rate or maintain the same data rate while halving the symbol rate. It has to be also noted that the shape of the DQPSK optical spectrum is identical to that of DPSK, but the DQPSK spectrum is compressed in frequency by a factor of two due to the halved symbol rate for transmission at fixed bitrate. The compressed spectrum is beneficial for achieving high spectral efficiencies in WDM system as well as for higher tolerance to chromatic dispersion. Longer symbol duration also makes DQPSK more robust to PMD [41].

DQPSK can be implemented in both RZ and NRZ format as well as DPSK. In [47], comparative analysis of NRZ and RZ-DQPSK for 112 Gbit/s DWDM transmission was conducted,when RZ-DQPSK turned out to be more resistant to chromatic dispersion and non-linearities. In [48], comparative simulation of different modulation formats (Non-return-to-zero (NRZ), return-to-zero (RZ), chirped RZ (CRZ), carrier suppressed RZ (CSRZ), duobinary, differential phase shift keying (DPSK), differential quadrature phase shift keying (DQPSK) and CSRZ-DQPSK) in 40 Gbit/s system at 100 km was performed. This simulation was focused on the effect of Polarization Mode Dispersion (PMD) and nonlinearity in terms of differential group delay. It was shown that RZ-DQPSK exhibits the lowest differential group delay with low as well as high PMD values. Due to such beneficial properties of DQPSK, this modulation format is being widely deployed in hybrid PON networks to improve data rate and transmission reach. In [49], comparative study of On-Off Keying and Differential Quadrature Phase Shift Keying in hybrid PON network was conducted. Utilization of DQPSK modulation scheme provided better results compared to the OOK for both low bit rate and high bit rate with EDFA, while enhancing achievable distance.

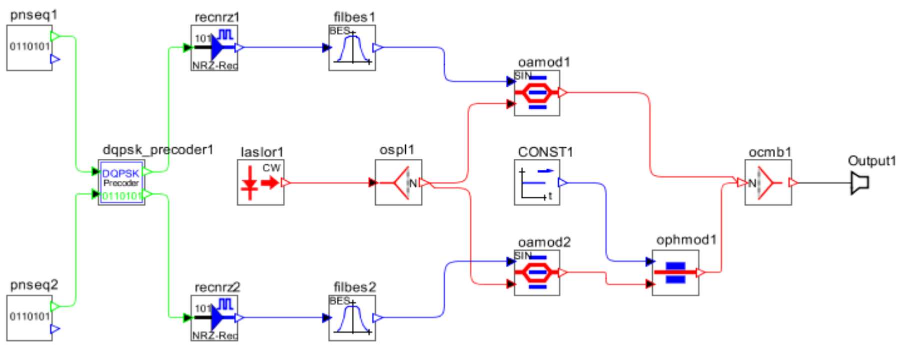

Figure 2.11: NRZ-DQPSK transmitter implementation

Fig. 2.11 depicts a transmitter setup of NRZ-DQPSK. The setup consists of continuously operating laser source, a splitter to divide the light into two paths of equal intensity, two MZMs operated as phase modulators, an optical $\pi/2$ phase shifter in one of the paths and a combiner to produce a single output signal [41].

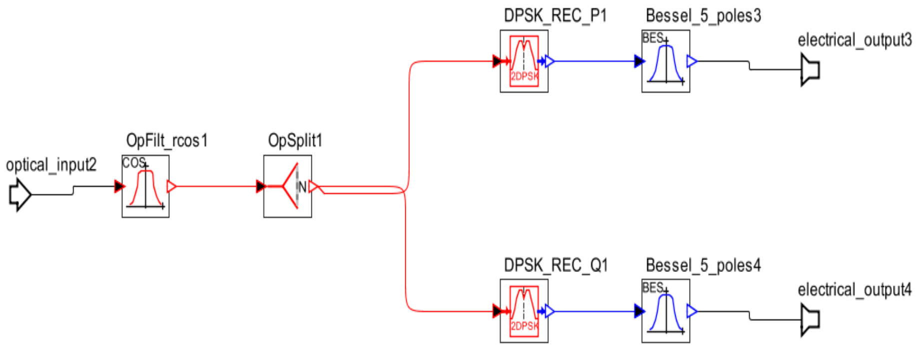

Figure 2.12: DQPSK receiver implementation

A model of the DQPSK receiver is shown in the figure 2.12. DQPSK receiver implementation consists of an optical band pass filter for the respective channel detection, optical splitter for in-phase and quadrature reception, balanced DPSK receivers in both branches, which convert in-phase and quadrature signals into electric current and electrical low pass filter in both branches for noise suppression.

2.5.4 Polarization Multiplexed Quadrature Phase Shift Keying

Polarization Divison Multiplex (PDM) doubles the feasible spectral efficiency by transmitting independent information in each of the two orthogonal polarization states. PDM requires polarization control at the receiver to separate the two polarization states. The main advantage is that, in a link not dominated by PMD or polarization dependent loss (PDL), PDM is a transparent multiplexing technique. The main drawback of PDM is the polarization sensitive detection required at the receiver. Besides adding complexity to the receiver, it reduces the PMD tolerance. The polarization sensitive detection can furthermore reduce the nonlinear tolerance in the case of WDM transmission because of XPM induced cross polarization modulation. With polarization sensitive detection, XPM results in a polarization dependent nonlinear phase shift. This nonlinear phase shift depends on the transmitted bit-sequence in co-propagating channels which leads to a noise-like change of the state of polarization, and hence depolarization [50].

As present DWDM systems with binary modulation formats are close to their limit in terms of spectral efficiency, further increase in spectral efficiency requires the use of multilevel modulation formats, which is challenging for long-haul transmission systems. Reduced system reach through higher Optical

Signal to Noise Ratio (OSNR) requirements combined with reduced tolerance to nonlinear impairments present a problem. On the other hand, multilevel modulation formats such as RZ-DQPSK have some clear advantages over binary modulation formats at the same data rate. Most notably, the narrower optical spectrum increase the tolerance toward cascaded optical filtering in a 50-GHz channel grid. Because of the lower symbol rate the chromatic dispersion and Polarization Mode Dispersion (PMD) tolerance are significantly higher in comparison to binary modulation formats.

Spectral efficiency of 1.6 bit/s/Hz using narrowband filtered RZ-DQPSK was reported. However, this results in relatively low cascaded filtering tolerances. The combination of both multilevel format (RZ-DQPSK) and Polarization Divison Multiplex (PDM) results in 4-bits/symbol modulation, which allows for a very narrow optical spectrum and long symbol period compared to binary modulation formats. This can be used to further increase the spectral efficiency to > 1.6-bit/s/Hz while maintaining sound filtering tolerances. Additionally, a high robustness against chromatic- and polarization-mode dispersion is obtained with respect to binary modulation [50].

The nonlinear tolerance of DWDM 21.4 Gbit/s RZ-DQPSK and 21.4 Gbit/s PM-RZ-DPSK modulation over an 800 km SSMF with 10.7 Gbit/s DPSK as a reference was examined in [51]. It was shown that with single channel transmission 21.4 Gbit/s RZ-DQPSK modulation suffers from an increased nonlinear impairments, which reduces the nonlinear tolerance significantly, whereas PM-RZ-DPSK modulation shows much better single channel performance. For multi-channel transmission only a small depolarization penalty is measured for 21.4 Gbit/s PM-RZ-DPSK modulation. The difference in nonlinear tolerance between 21.4 Gbit/s RZ-DQPSK and 21.4 Gbit/s PM-RZ-DPSK modulation is smaller for multi-channel transmission. In combination with the 1.5 dB sensitivity advantage for PM-RZ-DPSK 21.4 Gbit/s over 21.4 Gbit/s RZ-DQPSK modulation, PM-RZ-DPSK seems to be a better option for long haul transmission systems.

Higher robustness against nonlinear impairments of DPSK in comparison with DQPSK was confirmed in [52]. It was demonstrated by means of experiment that 43 Gbit/s PM-RZ-DPSK is more tolerant to nonlinear transmission impairments than 43 Gbit/s PM-RZ-DQPSK and enables an increase of 40 % in transmission reach by ultra long haul transmission system. However, in [50], it was shown that PM-RZ-DQPSK deployment in long haul transmission systems is viable, when 40 DWDM 85.6 Gbit/s channels in 50-GHz grid were successfully transmitted over 1700 km using PM-RZ-DQPSK.

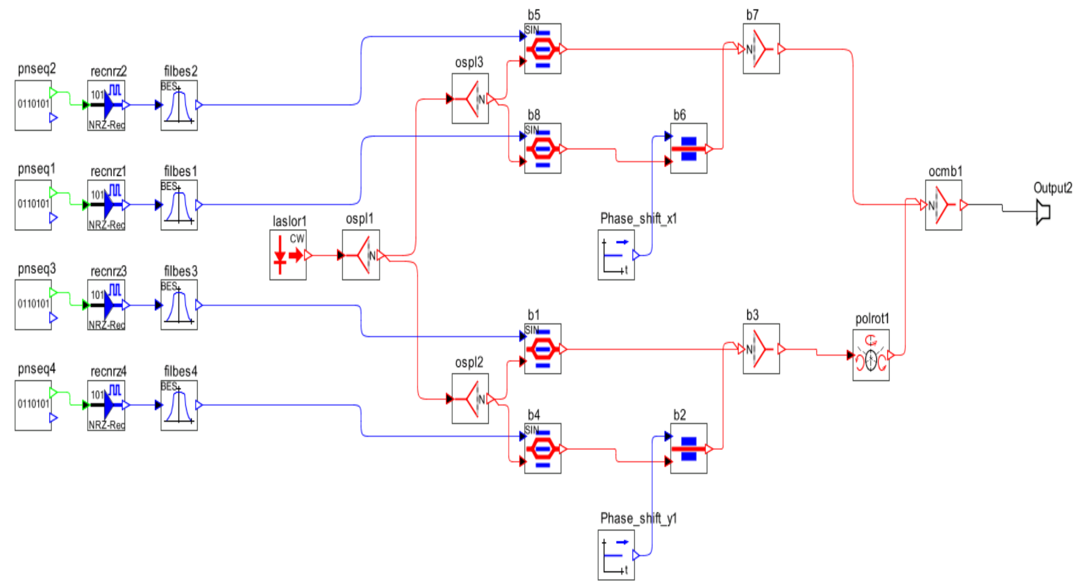

Figure 2.13: PM-NRZ-QPSK transmitter implementation

Fig. 2.13 shows the PM-NRZ-QPSK transmitter setup. Transmitter setup is basically made up of 2 QPSK transmitters with one transmitter transmitting with polarization shift of 180°. Laser beam is split into two branches. Each branch consists of 2 MZMs and phase modulator realizing QPSK modulation. However, in one branch polarization controller is present, executing rotation of polarization. As a result, QPSK signal with horizontal and vertical polarization is created. Both signals are then multiplexed and transmitted.

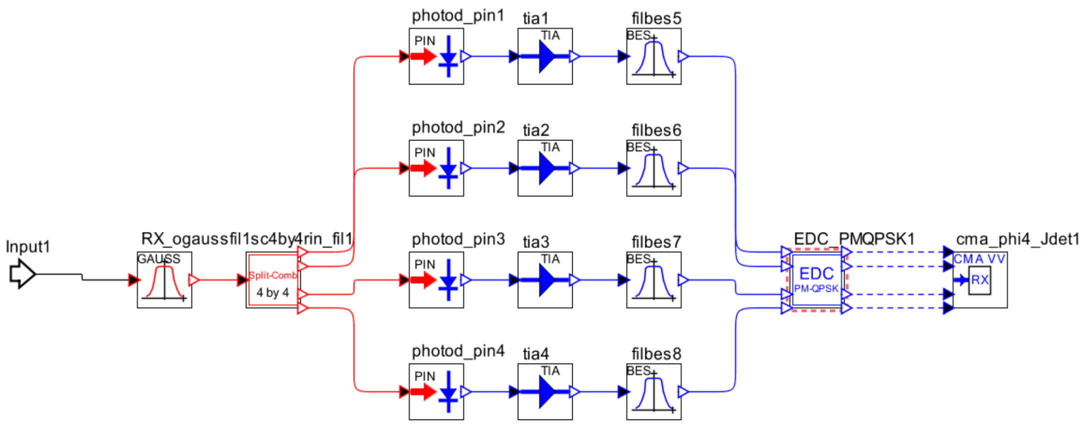

Figure 2.14: PM-QPSK receiver implementation

Figure 2.14 depicts the PM-QPSK receiver setup. The input optical signal is filtered by optical band pass filter to detect desired channel. Signal is then split into two polarization components by a polarization beam splitter. Two resulting components are sent to optical 90 degree hybrid circuit that enables extraction of phase, amplitude and polarization by performing interferences between a signal and a local oscillator. The output signal is proportional to the in-phase and quadrature components of received optical signals. Inserting photo-detectors at the four output ports one can obtain four electric current signals proportional to the mentioned four components of received optical signal, allowing coherent detection. Electronic Dispersion Compensator compensates for the chromatic dispersion and applies the same amount of compensation on signals deriving from both polarization components. Reception of coherent polarization multiplexed QPSK modulation is performed by memoryless blind receiver. This component recovers the Jones matrix of the channel and applies its inverse in order to separate data flows on orthogonal polarization. Then it estimates the average local-oscillator-to-signal phase in order to allow separation between in-phase and quadrature signals. When these steps are implemented, error counting is applied on the resulting 4 signals [65].

2.6 Channel coexistence

Previous sections were mainly focused on the phenomena, which generally occur in optical systems and have to be considered when designing an optical systems. Since this thesis deals with the coexistence of optical systems, this section is dedicated to interactions among different optical systems and how the resulting undesirable effects could be mitigated.

As discussed in Chapter 1, with higher line rates, physical layer impairments (PLIs) start to limit the performance of optical networks. The impact of these impairments strongly depends on the accumulated power and on the individual power of the other optical channels transported in parallel in the same fibre. The performance of Mixed Line Rates (MLR) is then affected by inter-channel and intra-channel interference. There have been number of works investigating the system performance of MLR under different modulation formats and the effect of coexistence.

In [53], comparative simulation of MLR consisting of 11 channels (3 x 40 Gbit/s in the cenre and 4 surrounding channels 10 Gbit/s NRZ-OOK on either side) under different modulation formats in presence of non-linear impairments and channel spacing was performed. It was observed that the performance of Duo-binary optical modulation scheme is superior to NRZ-OOK and DPSK schemes at 40 Gbit/s transmission at fixed grid as well as flexi grid WDM scenario due to its smaller modulation bandwidth. Impact of channel plan and dispersion map on hybrid DWDM transmission of 42.7 Gbit/s DQPSK and 10.7 Gbit/s OOK on 50 GHz grid was examined in [54]. It was found that Cross-Phase Modulation (XPM) from OOK channels is a dominant source of nonlinearity impairment for co-propagating DQPSK channels. It was shown that in the case of one DQPSK channel among seven NRZ-OOK channels or hybrid interleaved NRZ-OOK and RZ-DQPSK system XPM causes severe degradation of system performance. However, the effect of XPM could be mitigated by residual dispersion, as large residual dispersion provides large channel walk-off. Another way how to limit XPM penalty is a suitable channel plan, namely a guard band between NRZ-OOK channels and RZ-DQPSK channels, which however, reduces system capacity and imposes inflexibility in the channel plan.

In [55], upgrade of existing 10 Gbit/s infrastructure to channel data rates of 40 Gbit/s and 100 Gbit/s is elaborated, while comparing modulation formats in terms of PMD tolerance, dispersion tolerance, inter-channel interference or filtering tolerance. Transmission of a 111 Gbit/s DP-DQPSK signal over 1040 km field-deployed fibre together with different types of neighboring channels by means of an experimental setup was shown in [56]. Two sets of neighboring channels were launched next to the 111 Gbit/s PM-RZ-DQPSK channel. The first set includes 10 x 10.7 Gbit/s OOK channels, at 50 GHz spacing from the 111 Gbit/s channel. The second consists of two 43 Gbit/s DPSK channels, placed around the 111 Gbit/s channel with 50 GHz spacing. Around the 43 Gbit/s channels, 8 x 10.7 Gbit/s OOK channels are placed. The results show a strong Cross-Phase Modulation (XPM) influence from the OOK channels on the 111 Gbit/s channel. However, this influence can be significantly reduced by carefully choosing the launch power levels for these neighbors. The 43 Gbit/s channels, on the other hand, show some degradation in the performance for a certain level of launch power level. This performance degradation is due to both XPM and linear crosstalk on the 43 Gbit/s channels from the wide spectrum of the 111 Gbit/s channel. The 10.7 Gbit/s OOK channels have better tolerance to XPM, as well as a narrower bandwidth which means that they suffer less from any linear crosstalk.

Similar experiment was conducted in [57], where the same sets of neighboring channels as in [56] were analyzed. It was confirmed that the impact of 10.7 Gbit/s channels on the 111 Gbit/s channel is higher than that of 43 Gbit/s channels due to stronger XPM effects from OOK-modulated 10.7 Gbit/s channels. Besides this, PMD tolerance tests on the 111 Gbit/s channel was performed, while sustaining at least 23 ps mean Differential Group Delay (DGD) for error-free operation, owing to strong digital processing in the coherent receiver.

Chapter 3

Methods

3.1 Time Domain Split-step

Optsim simulation software was used to perform simulations. Simulations performed by Optsim software are based on Split-step method to perform the integration of the fibre propagation equation

$$\frac{\partial A(t,z)}{\partial z} = \{L + N\}A(t,z) \tag{3.1}$$

where $A(t,z)$ is the optical field, L is the linear operator responsible for dispersion and other linear effects and N is the non-linear operator that accounts for the Kerr effect and other non-linear effects like SRS or pulse self-steepening. The Split-Step integration algorithm works by applying separately L and N to $A(t,z)$ over small spans of fibre Δz. The error deriving from separating the effects of L and N goes to zero faster than $(\Delta z)^2$.

As a linear operator, L is fully characterized by its impulse response h(t) and the mathematically correct way to compute its effect on A(t,z) is via a convolution product in time. Time Domain Split-step (TDSS) calculates L in the time domain by calculating the convolution product in sampled time, which can be written as

$$TDSS \Rightarrow A_L[n] = A[n] * h[n] = \sum_{k=-\infty}^{\infty} A[k]h[n-k] \tag{3.2}$$

Although Frequency Domain Split-step can be implemented much easier, the circular convolution it applies will introduce aliasing, which is an error intrinsic to the method, thus it cannot be avoided. As a result, TDSS performs better in many aspects, such as immunity against aliasing errors, accurate differential group delay or fullband simulation, at the cost of implementation complexity [58].

3.2 Monitors

3.2.1 BER

Evaluation of system performance is performed by means of Bit Error Rate (BER) and Q-factor. BER is the number of bit errors (N_{error}) divided by the total number of transferred bits (N_{total}) during a certain time interval and can be calculated as follows

$$BER = \frac{N_{error}}{N_{total}} \tag{3.3}$$

The most commonly used techniques in the communications system simulations are direct error counting, semianalytical techniques and the various forms of Gaussian approximations based on the estimation of the moments of the received signals. Of all these techniques, direct error counting is seldom used in the simulation of the optical systems, because for BER close to 10^{-9} the simulation of at least 10^{10} bits is required to achieve a reasonable accuracy, and would thus need an prohibitively large CPU time even for extremely simple link setups.

Although semianalytical approach is very accurate, need for exact knowledge prevents it from deployment in many cases. Therefore the most commonly used approach is the simulation of the propagation of signal and noise along the link using estimation of moments of a received signal.

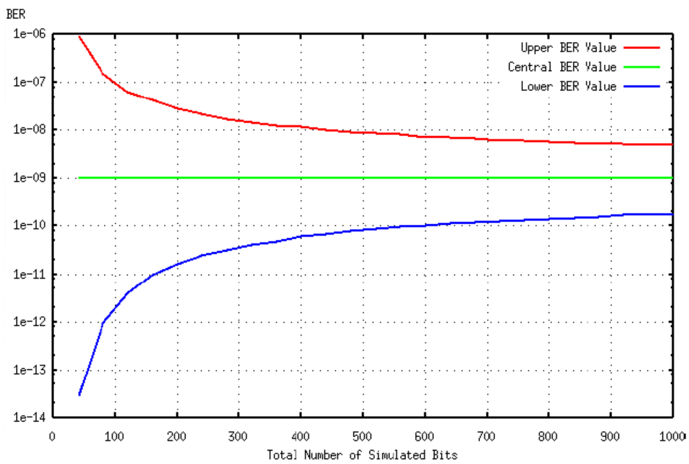

Figure 3.1: BER estimate range (95% confidence interval) for a nominal BER $= 10^{-9}$, taken from: [58]

As fig. 3.1 shows, the accuracy of BER estimation rises, as number of simulated bits increases. But after a certain threshold the accuracy rises very slowly. As it can be shown by direct comparison, the confidence interval at BER around 10^{-9} is given by roughly ± 1 order of magnitude for 512 simulated bits [58].

3.2.2 Q-factor

According to ITU recommendation [59], Q-factor is defined for a digital transmission signal as Signal to Noise Ratio (SNR) at the receivers decision circuit and is expressed as

$$Q = \frac{\mu_1 - \mu_0}{\sigma_1 + \sigma_0} \tag{3.4}$$

where μ_1,σ_1(μ_0,σ_0) are the mean values and the standard deviations of the received signal at the sampling instant when logical 1(0) is transmitted with the assumption that ones and zeros are uncorrelated and additive noise is statistically independent from the signal. Fig. 3.2 shows an illustration of the eye diagram and how could the mean values and standard deviations of logical 1 and 0 be obtained from this diagram.

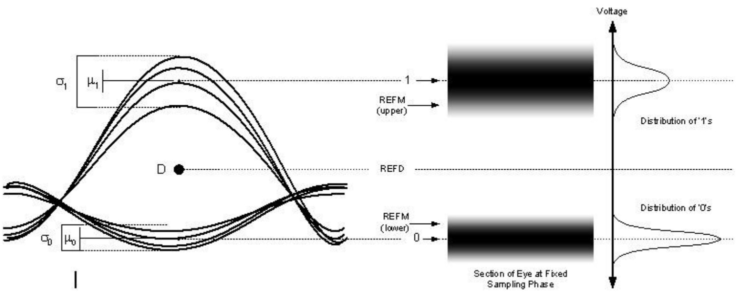

Figure 3.2: Illustration of eye diagram, taken from: [60]

Mathematical relation between BER and Q-factor shows following formula

$$BER = \frac{1}{2} erfc\left(\frac{Q}{\sqrt{2}}\right) \tag{3.5}$$

where

$$erfc(x) = \frac{2}{\sqrt{\pi}} \int_x^{\infty} e^{-u^2}\, du \tag{3.6}$$

Q-factor estimation is as well as BER estimation subject to error, when the accuracy varies with number of simulated bits. Fig. 3.3 depicts dependence of Q-factor estimation accuracy on number of simulated bits. It can be seen that approximately 500 bits are required in order to have a Q-factor confidence intervals of ±1dB. On the basis of relation between accuracy of BER and Q-factor estimation and number of simulated bits I decided to simulate 800 bits to achieve reasonably accurate results.

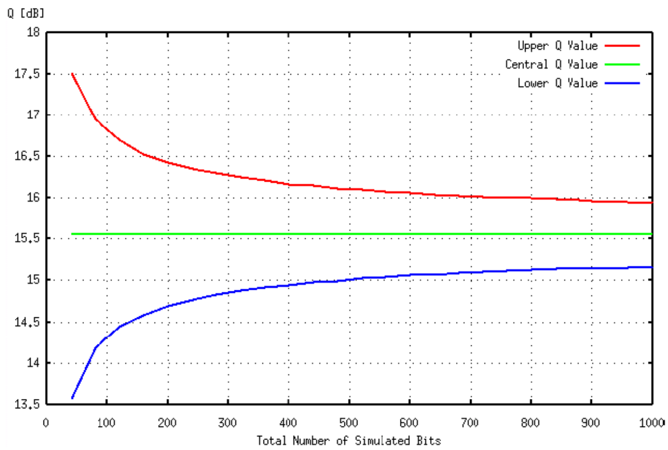

Figure 3.3: Q-factor estimate range (95% confidence interval) for a nominal Q=6 (15.56 dB), corresponding to BER= 10 − 9,taken from: [58]

3.3 Simulation layout

A number of simulation layouts had to be designed in order to simulate the impact of interactions in a DWDM optical system, where multiple modulation formats coexist. However, all of them are based on a general layout depicted in the fig. 3.4 with P2P topology.

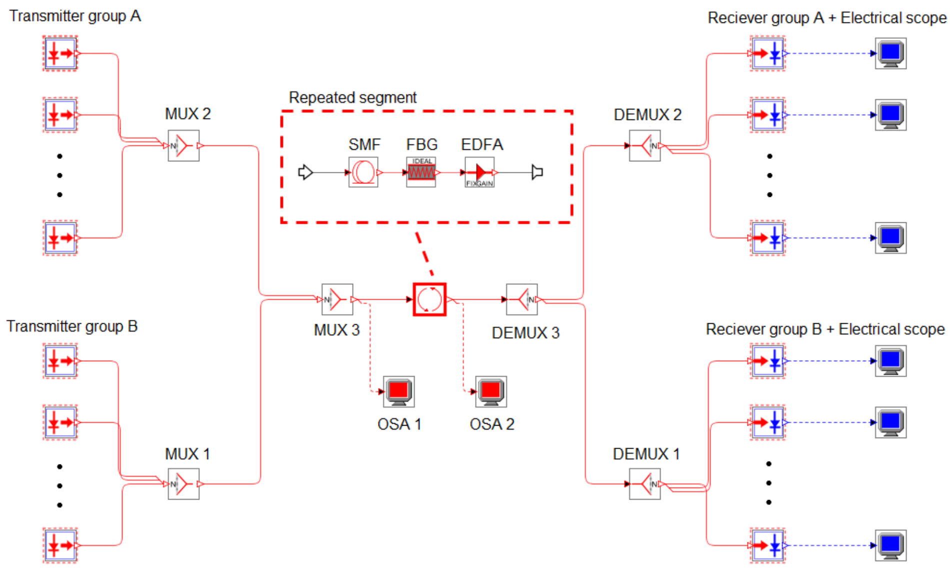

Figure 3.4: General simulation layout

The general layout could be divided into 3 separate sections. First section called "Transmitter group" represents an array of transmitters. Transmitter blocks differ in their design depending on the modulation format employed in the simulation. Transmitter implementation of each modulation format used in this thesis was discussed in the section 2.5. Channel spacing varies with respective simulation, while following ITU-T G.694.1 recommendation. Each channel is filtered by optical band pass filter with bandwidth corresponding to the channel spacing and multiplexed in an ideal optical combiner labelled as “MUX”. Example of a transmitter array is shown in figure 3.5.

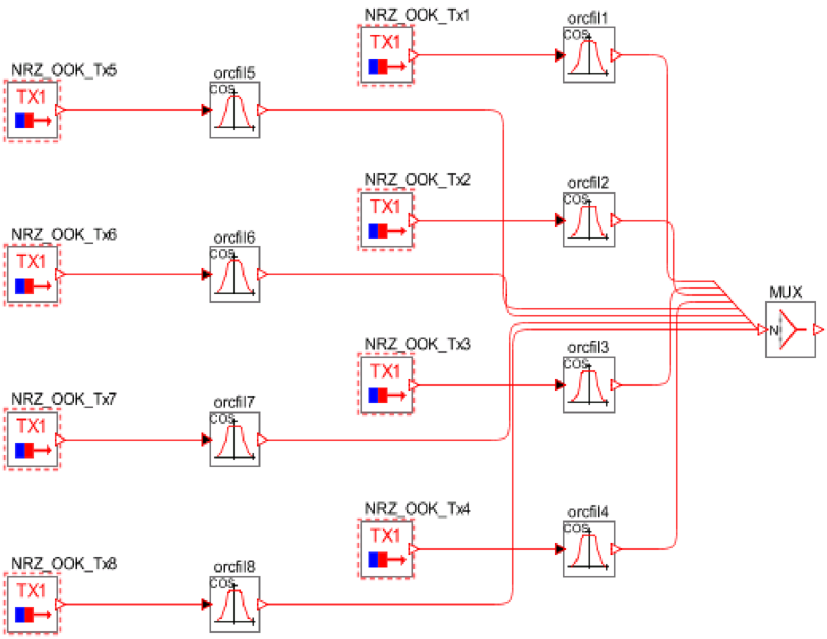

Figure 3.5: DWDM transmitter array with NRZ-OOK transmitter blocks

Another part is a repeated segment. Repeated segment consists of an optical fibre and optionally compensating elements such as Fibre Bragg Grating and Erbium Doped Fibre Amplifier for chromatic dispersion compensation and loss of an optical fibre compensation, respectively. Compensating dispersion of the grating and gain of the amplifier are adjusted so that desired properties of the optical link are reached. Figure 3.6 illustrates such a repeated segment. Optical fibre used in the simulations is an ITU-T recommendation G.652 compliant single mode fibre. Its parameters are stated in the table 3.1.

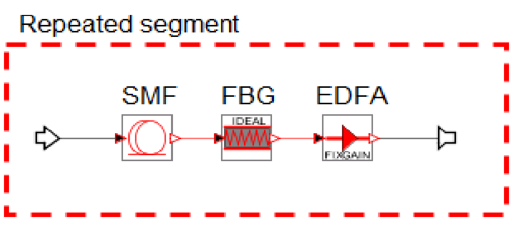

Figure 3.6: Repeated segment

The last section, “Receiver group + Electrical scope”, is made up of receivers and electrical measurement components. Receiver structure depends

Parameter	Value
Maximum Attenuation (at 1550 nm)	0.2 dB/km
Dispersion (at 1550 nm)	16 ps/(nm · km)
Dispersion slope (at 1550 nm)	0.07 ps/(nm^2 · km)
Polarization mode dispersion (PMD)	$\leq$ 0.1 ps/$\sqrt{\text{km}}$
Effective core area (at 1550 nm)	80 μm^2

Table 3.1: Optical fibre specifications

on the modulation format utilised in the simulation. Basically, the main components of the receiver is a PIN photodiode and electrical low pass filter. Optical band pass filter cuts out the respective channel from the spectrum after demultiplexing and reduces Amplified Spontaneous Emission (ASE) introduced by the amplifiers. Photodiode receives an optical signal, which is then converted into the electrical domain. Noise of the electrical signal is also suppressed by the low pass filter. However, cut-off frequency of the low pass filter cannot be too low, because the spectrum of the signal would be deformed and thus BER would increase. Detailed receiver implementation of each modulation format used in this thesis was discussed in the section 2.5. System performance is evaluated on the basis of Q-factor and Bit Error Rate (BER) as stated in the section 3.2.1. These values provide electrical scope or BER estimator in Optsim simulation software. Example of a receiver array depicts figure 3.7.

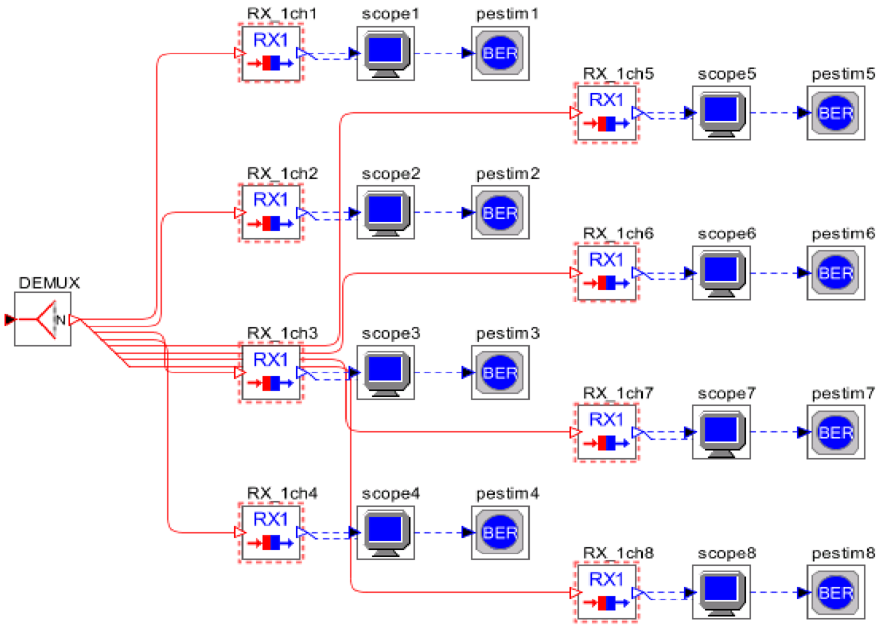

Figure 3.7: DWDM receiver array with OOK receiver blocks

Chapter 4

Simulation results

4.1 Signal recovery and regeneration interval

4.1.1 Individual modulation formats

Simulated optical network reach was 400 km, which is a medium-reach optical link corresponding to the national network reach. This network is made up of repeated segments, which contain optical fibre with various length, chromatic dispersion compensating element and Erbium Doped Fibre Amplifier. Length of the optical fibre was varied between 50 and 100 km with step equal to 5 km. If the number of repeated segments could not be an integer, another repeated segment of remaining length was added.

As the transmission quality deteriorates due to the attenuation and chromatic dispersion while propagating through an optical fibre, the signal needs to be regenerated. This is done in the repeated segments, where the attenuation of the optical fibre is fully compensated in EDFA and so is chromatic dispersion in Fibre Bragg Grating. This process depicts figure 4.1.

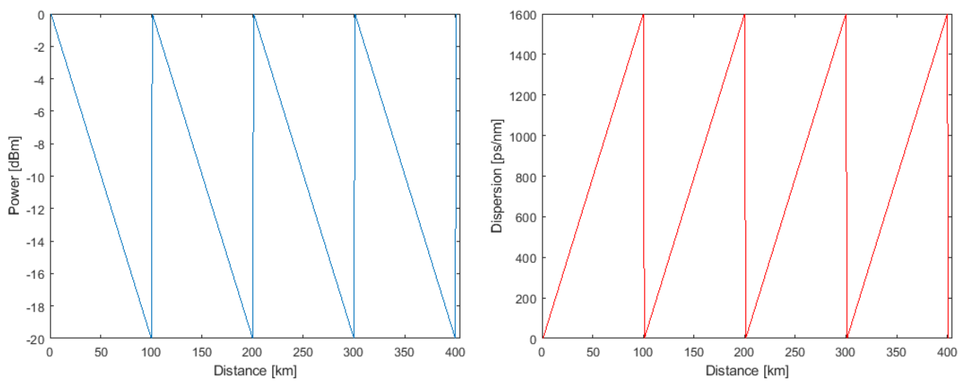

(a) : Attenuation compensation **(b) :** Chromatic dispersion compensation

Figure 4.1: Signal regeneration

The default system is made up of fifteen 10 Gbit/s channels with NRZ-OOK modulation on 100 GHz channel grid symmetrically distributed around pilot frequency equal to 193.1 THz. Launch power level of the DWDM system was set to 0 dBm by means of fixed-output power amplifier. Channels are multiplexed in an ideal combiner, regenerated in each repeated segment, demultiplexed in an ideal optical splitter and detected in the respective receiver. In the default system, post compensation of chromatic dispersion was utilized. Simulation layout of the the default system is depicted in figure 4.2. The purpose of the first simulation was to observe the process of signal degradation as the interval between repeated segments gradually prolonged from 50 to 100 kilometres with step equal to 5 kilometres. Resulting Bit Error Rate (BER) and Q-factor were then measured and plotted in a graph. Values plotted in the graphs correspond to the worst channel values obtained by the simulation.

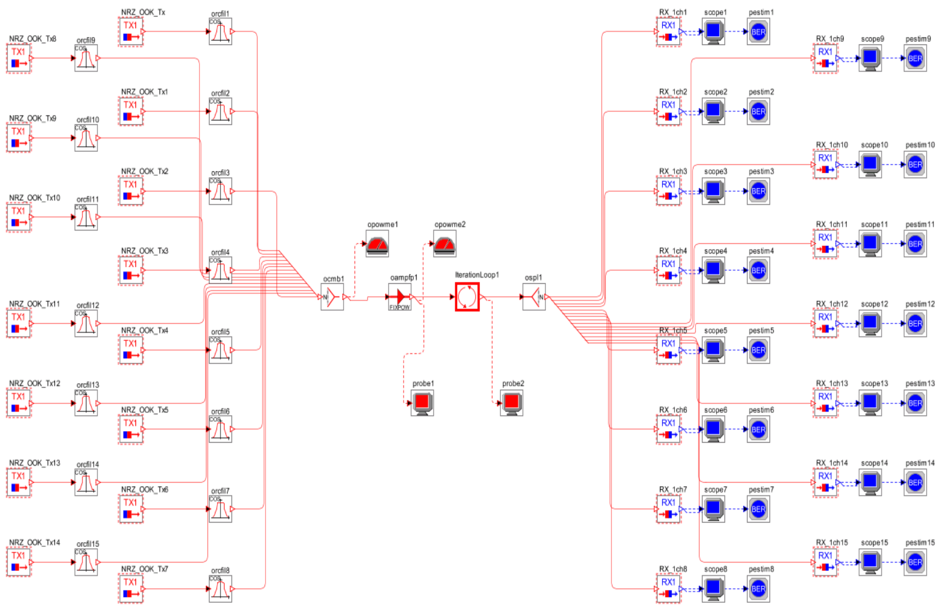

Figure 4.2: Default DWDM system with 10 Gbit/s NRZ-OOK channels

Before I studied potential cross-talks and interactions between different modulation formats, I tested each modulation format separately with the same test conditions mentioned above. Besides legacy 10 Gbit/s NRZ-OOK also 20 Gbit/s NRZ-DPSK and 40 Gbit/s NRZ-DQPSK were simulated. Simulation results are shown in figure 4.3a and figure 4.3b.

Looking at the graphs one can see, signal quality clearly deteriorates, as the regeneration interval increases, in other words, Bit Error Rate (BER) increases with increasing regeneration interval and Q-factor decreases with increasing regeneration interval regardless of the modulation format utilised. Although more Erbium Doped Fibre Amplifier (EDFA) add more noise to the optical link, it is apparently outweighed by more frequent signal regeneration. However, the more regeneration segments are present in the optical link, the more expensive whole optical systems gets.

Then it is possible to observe that smaller regeneration interval is necessary to guarantee certain transmission quality if the legacy 10 Gbit/s NRZ-OOK is meant to be replaced by more advanced modulation format with higher bitrate. Threshold for the quality transmission was set at BER= 10^{-10}, which corresponds to Q-factor ≈ 16.1 dB. This quality threshold was chosen in accordance with the ITU-T Recommendation G.Sup39 [61]. Figure 4.3 shows dependence of signal degradation on regeneration interval in case of separate systems.

In case of legacy 10 Gbit/s NRZ-OOK it is clear that BER threshold is exceeded only if the regeneration interval is equal to 100 km. However, in contrast to other modulation formats deployed, the process of degradation is steepest. For example 40 Gbit NRZ-DQPSK is at 65 kilometres already on the edge of an allowed error rate, nevertheless the curve is then a lot more flat and the quality worsens a lot slower than in case of NRZ-OOK.

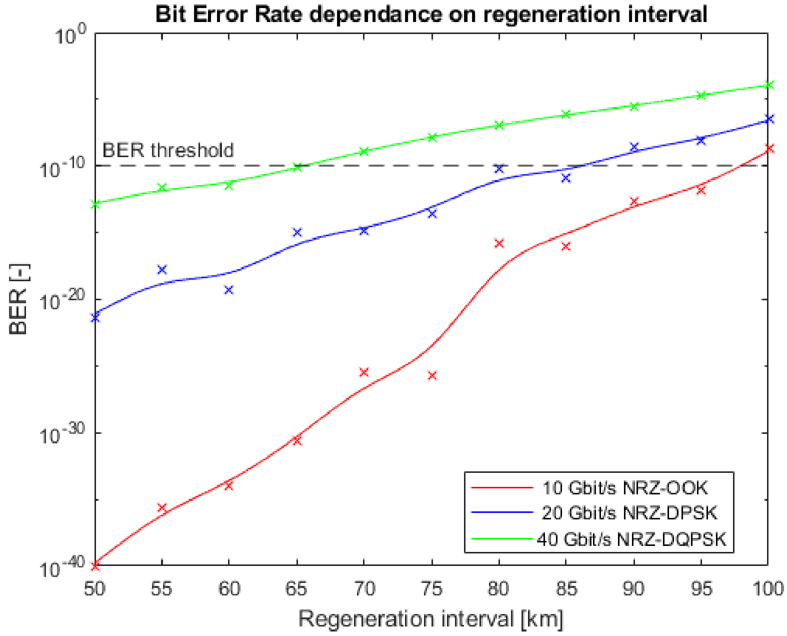

(a) : BER vs regeneration interval

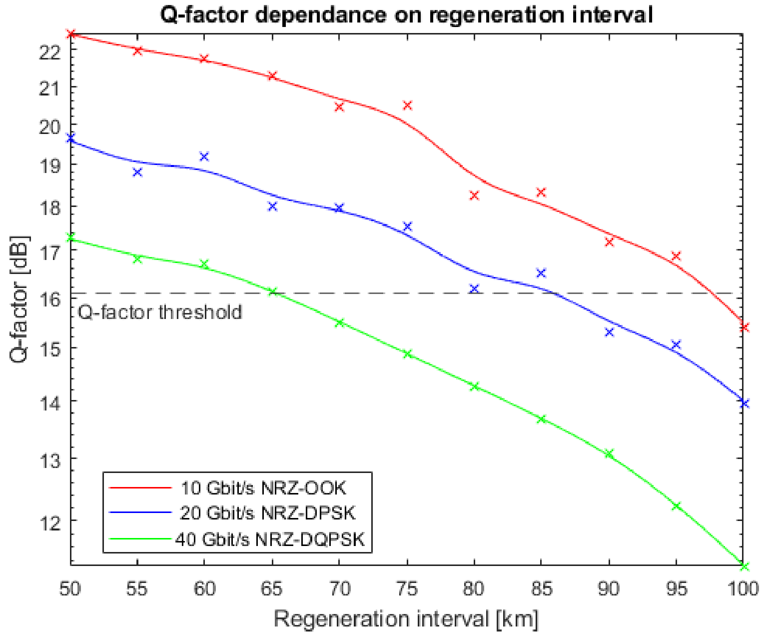

(b) : Q-factor vs regeneration interval

Figure 4.3: Signal degradation dependence on regeneration interval in case of separate systems

4.1.2 Coexistence of modulation formats

In this subsection I examined the scenarios, when multiple modulation formats coexist and how they affect each other. The simulation conditions are the same as they were in the previous subsection. There are 15 channels on the 100 GHz grid with the launch power level equal to 0 dBm. Signal is regenerated in repeated segments consisting of EDFA and FBG in post compensation setup.

First simulation investigates coexistence of 10 Gbit/s NRZ-OOK and 20 Gbit/s NRZ-DPSK. This simulation scenario could serve as an example, how would these two modulation formats coexist in a transitional period, when the network provider would like to replace legacy 10 Gbit/s NRZ-OOK with 20 Gbit/s NRZ-DPSK. Channel groups are organised in such a way that even channels correspond to the 20 Gbit/s NRZ-DPSK format (group B) and odd channels correspond to 10 Gbit/s NRZ-OOK format (group A). Channel distribution in the input spectrum is shown in fig. 4.4. Similarly to the previous simulation, BER and Q-factor values were recorded for the worst channels of either channel group and plotted in a graph. Simulation results of coexistence of 10 Gbit/s NRZ-OOK and 20 Gbit/s NRZ-DPSK in DWDM system are shown in figure 4.5.

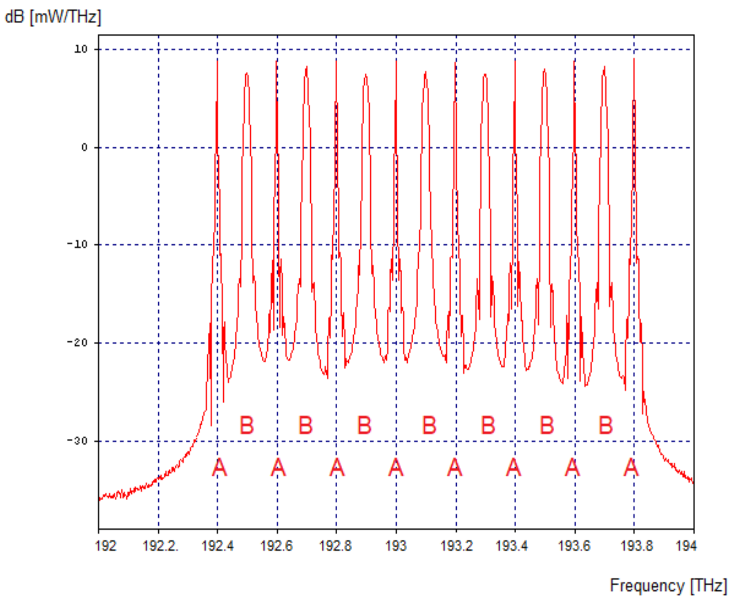

Figure 4.4: Channel distribution in the OOK-DPSK system

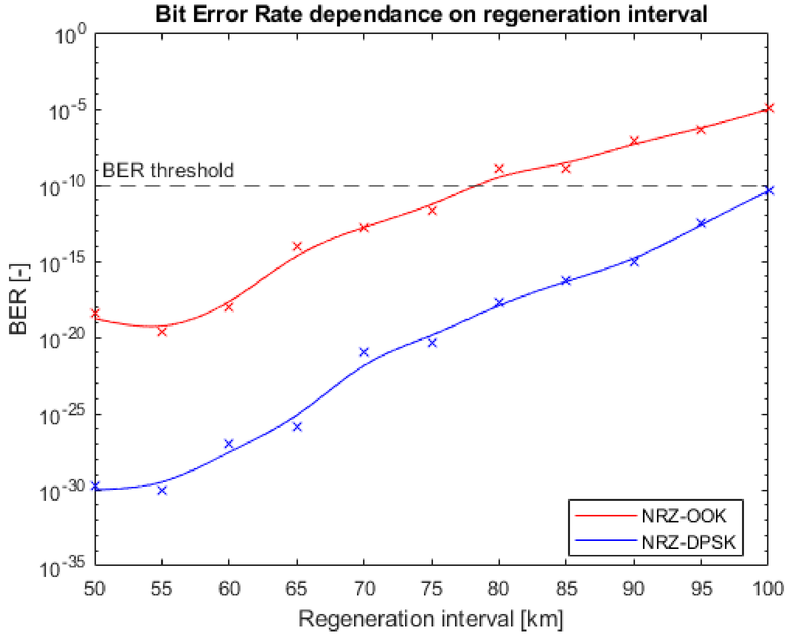

(a) : BER vs regeneration interval

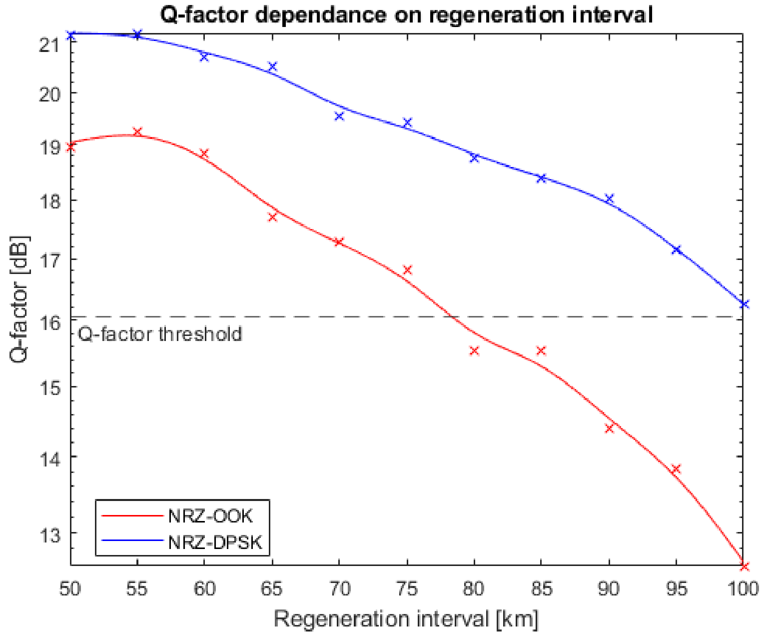

(b) : Q-factor vs regeneration interval

Figure 4.5: Signal degradation dependence on regeneration interval in case of coexistence of NRZ-OOK and NRZ-DPSK

Comparing figure 4.3 and figure 4.5 one can see that 20 Gbit/s NRZ-DPSK outperforms 10 Gbit/s NRZ-OOK, when both modulation formats coexist. NRZ-OOK channels clearly suffer from inter channel interference more than 20 Gbit/s NRZ-DPSK. Analysing the maximal regeneration interval in the case of legacy 10 Gbit/s NRZ-OOK system, necessary regeneration interval to guarantee required quality was maximally 95 kilometres. If NRZ-OOK channels coexist with 20 Gbit/s NRZ-DPSK channels, maximal regeneration interval drops to 75 kilometres. As a result, if the network provider decides to operate both systems simultaneously, he has to count on this restriction and shorten regeneration interval to ensure the required transmission quality.

Second simulation investigates possibility of coexistence of 10 Gbit/s NRZ-OOK with 40 Gbit/s NRZ-DQPSK. Default simulation conditions are the same as they were in the previous case of coexistence of NRZ-OOK and NRZ-DPSK. Channel groups are organised in such a way that even channels correspond to the 40 Gbit/s NRZ-DQPSK format (group B) and odd channels correspond to 10 Gbit/s NRZ-OOK format (group A). Channel distribution is shown in figure 4.6, while dependence of BER and Q-factor on the regeneration interval is depicted in figure 4.7a and 4.7b respectively.

Looking at the measured data, it is clear that NRZ-OOK suffers greatly due to inter channel interference, while NRZ-DQPSK performs even better than in the case of a separate system. As well as in the case of coexistence of NRZ-OOK and NRZ-DPSK, modulation format which limits the regeneration interval, is the legacy 10 Gbit/s NRZ-OOK system. Consequently, regeneration interval required to transmit data with required BER fell sharply to 65 kilometres, whereas in the separate 10 Gbit/s NRZ-OOK system up to 95 kilometres were sufficient. As a result, network provider has to bear in mind that coexistence of different modulation formats brings about crosstalks, which result in shortening of the regeneration interval, which is sufficient enough to guarantee the quality measure.

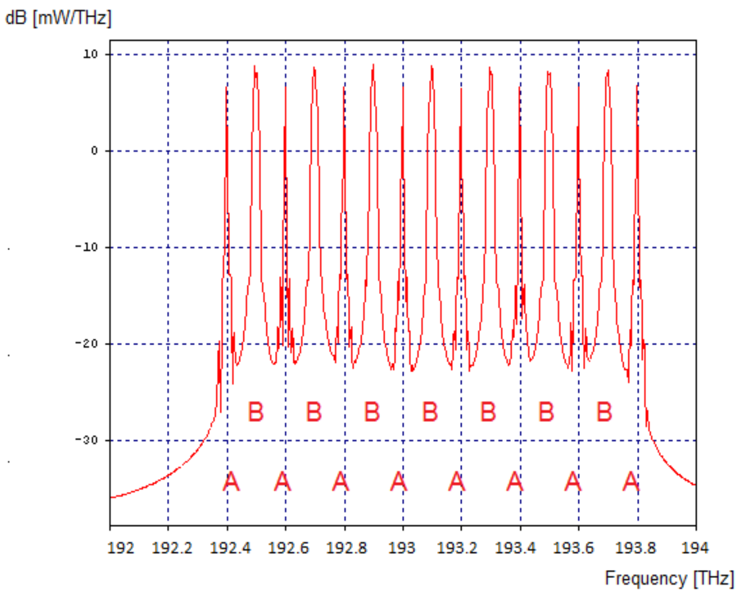

Figure 4.6: Channel distribution in the OOK-DQPSK system

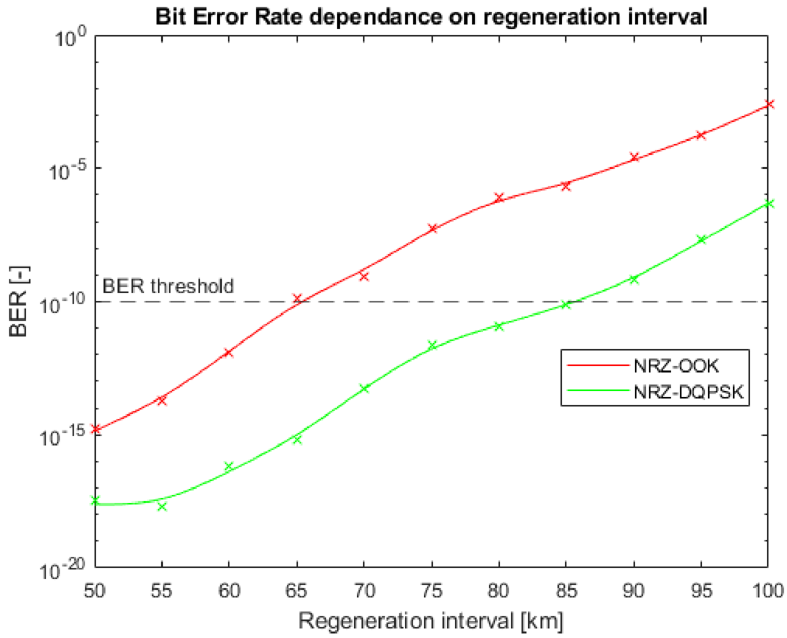

(a) : BER vs regeneration interval

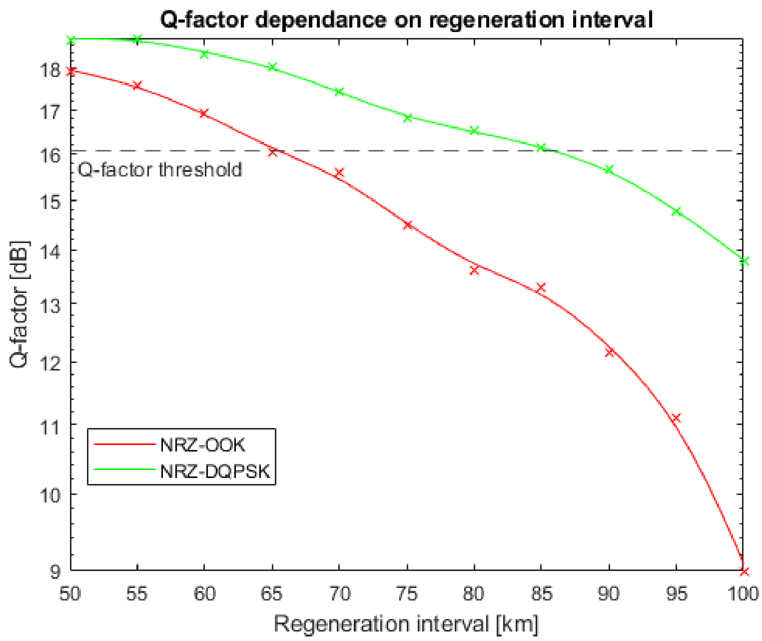

(b) : Q-factor vs regeneration interval

Figure 4.7: Signal degradation dependence on regeneration interval in case of coexistence of NRZ-OOK and NRZ-DQPSK

In the last simulation setup, coexistence of all modulations format previously deployed, thus coexistence of 10 Gbit/s NRZ-OOK, 20 Gbit/s NRZ-DPSK and 40 Gbit/s NRZ-DQPSK, was investigated. Default simulation conditions remain the same as in the previous simulation scenarios. However, channel distribution differs. There are still 15 channels on the 100 GHz grid, where odd channels correspond to 10 Gbit/s NRZ-OOK channels (group A) and even channels are split into 2 alternating groups (group B and group C). Group B corresponds to the 20 Gbit/s NRZ-DPSK and group C corresponds to the 40 Gbit/s NRZ-DQPSK. Channel distribution illustrates figure 4.8. BER and Q-factor values were recorded and plotted in a graph, which depicts figure 4.9

By observing the graphs one can see that as well as in the previous simulation results, 10 Gbit/s NRZ-OOK showed the worst results, when BER threshold is exceeded at 75 kilometres. This result is, however, better comparing coexistence of OOK-DQPSK, where BER threshold was exceeded already at 65 kilometres, see figure 4.7. When comparing figure 4.5 and figure 4.9 , it is possible to observe that shape of the curve of 10 Gbit/s NRZ-OOK is quite similar as well as the sufficient regeneration interval (75 kilometres in case OOK-DPSK coexistence). On the basis of this it can be concluded that 20 Gbit/s NRZ-DPSK channels significantly impact NRZ-OOK channels in terms of channel interference. NRZ-DPSK performed a bit worse in comparison with the OOK-DPSK scenario, nevertheless, sufficient regeneration interval was still quite long (95 kilometres). NRZ-DQPSK achieved similar results in terms of sufficient regeneration interval (90 kilometres), but more importantly, required regeneration interval significantly extended comparing OOK-DQPSK scenario, see figure 4.7. Another interesting point is that DPSK and DQPSK curves are quite far from each other at the beginning. However, at longer distances they somewhat converge, when difference in BER at 100 kilometres is almost negligible.

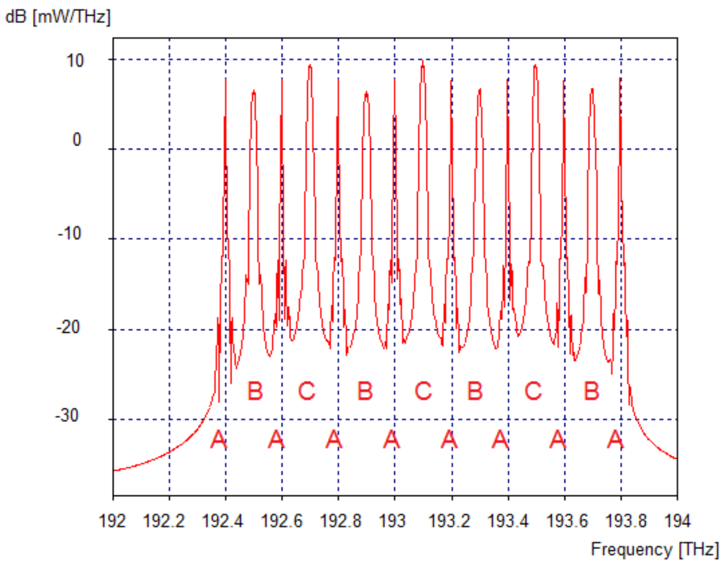

Figure 4.8: Channel distribution in the OOK-DPSK-DQPSK system

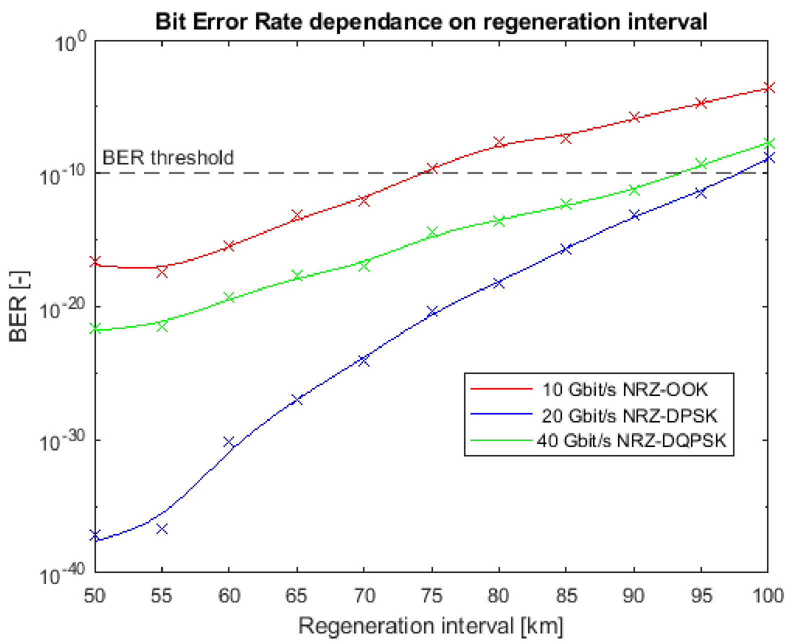

(a) : BER vs regeneration interval

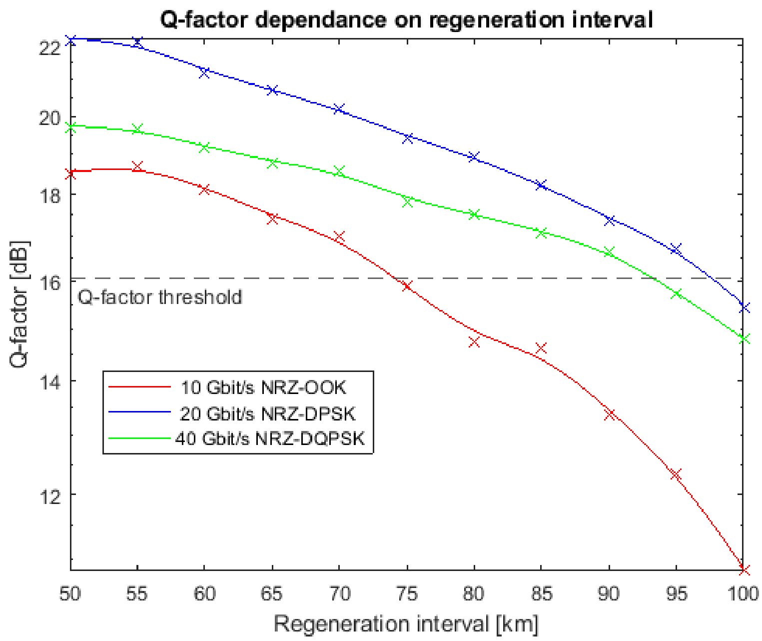

(b) : Q-factor vs regeneration interval

Figure 4.9: Signal degradation dependence on regeneration interval in case of coexistence of NRZ-OOK, NRZ-DPSK and NRZ-DQPSK

4.2 Performance of modulation formats in the PON scenario

In this section, I investigated performance of three modulation formats in the PON scenario, in which neither optical amplifiers nor dispersion compensating elements are present. I followed ITU-T Recommendation G.G.9804.1 for higher speed passive optical networks that operate at speeds of over 10 Gbit/s per channel, while maximum fibre distance is at least 20 kilometres [62]. Maximal fibre length was set at 40 kilometres, as this is a common fibre distance in WDM-PON networks, see [63]. Each modulation format was at first tested separately with 8 Optical Network Units (ONUs) and 8 Optical Line Termination (OLT) modules. Each ONT and OLT module has reserved wavelengths for upstream transmission and downstream transmission, respectively. As a result, this network architecture could be regarded as a set of point-to-point links. Based on that, this simulation layout consists of 16 channels with channel spacing equal to 100 GHz. Launch power level is equal to 0 dBm. Unlike simulation layouts utilised in the previous section, this simulation layout does not include any regeneration segments, where signal recovery is performed. Once the channel multiplexing is done, the signal propagates through an optical fibre without dispersion or attenuation compensation. Channels are then split in an ideal splitter and received in the respective receiver with an optical band bass filter, which enables detection of the corresponding wavelength. BER and Q-factor values are then recorded. These values are plotted in a graph, which shows dependence of BER and Q-factor on fibre length for each modulation format. This graph depicts figure 4.10.

As one could see, 10 Gbit/s NRZ-OOK totally outperformed more advanced modulation format 20 Gbit/s NRZ-DPSK and 40 Gbit/s NRZ-DQPSK in this setup. While NRZ-OOK curve did not exceed BER threshold even at 40 kilometres, in case of NRZ-DPSK and NRZ-DQPSK it is around 20 and 9 kilometres, respectively. Consequently, simulation results confirm theoretical assumptions, which favour NRZ-OOK in a short reach optical systems in comparison with more advanced modulation formats. It is also of interest that by each modulation format there is a certain threshold when exceeding it BER starts to rapidly increase and Q factor decrease. It is important to mention that BER equal to $1 \cdot 10^{-40}$ is the lowest possible BER that could be obtained in the simulation. Nevertheless, one cannot say that if this value is obtained with no fibre present, receiver and transmitter setup is ideal. However, this is difficult to optimize, since it is not possible to obtain lower BER.

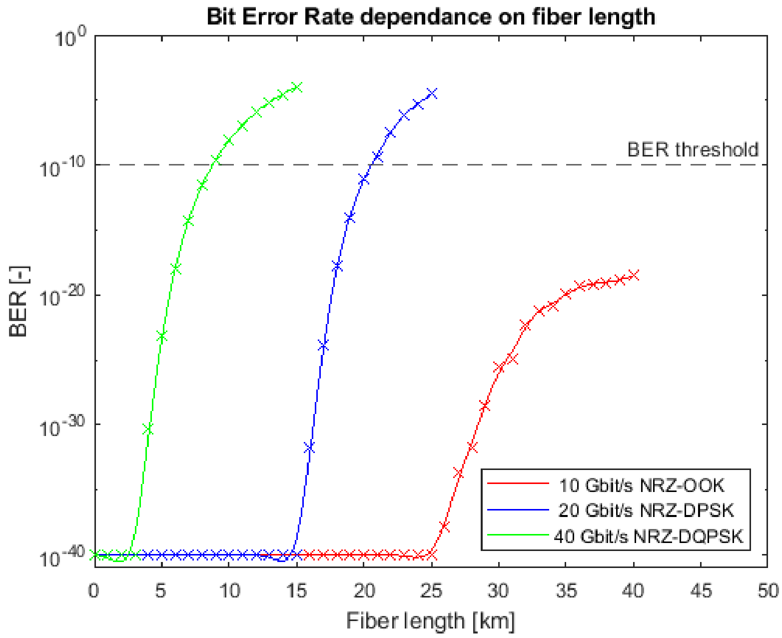

(a) : BER vs fibre length

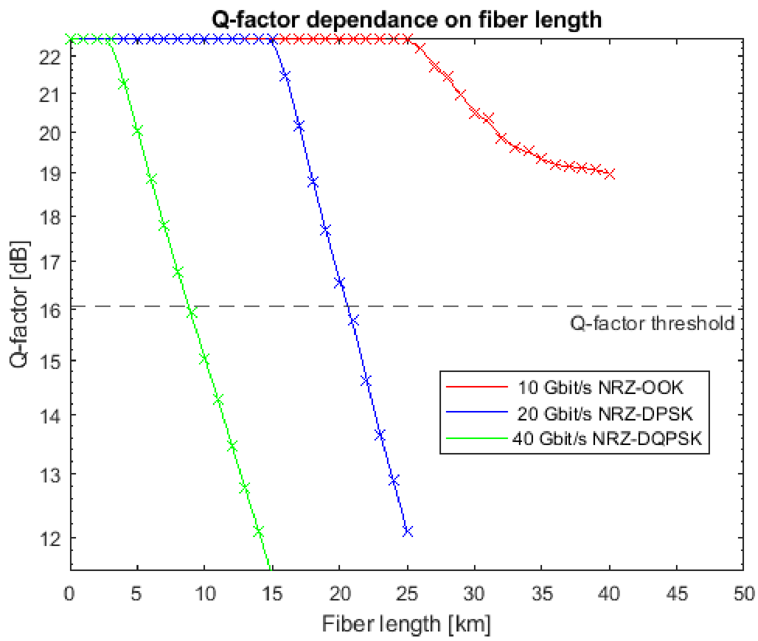

(b) : Q-factor vs fibre length

Figure 4.10: Signal degradation dependence on fibre length in case of separate systems in PON setup

To better illustrate the effect of signal degradation, eye diagrams for each modulation format are displayed. Eye diagrams for 10 Gbit/s NRZ-OOK at various fibre lengths are shown in figure 4.11. One can see that eye patter gradually closes, as the length of the fibre increases. Conversely an open eye pattern corresponds to the minimal signal distortion. It is possbile to observe that eye diagram of 10 Gbit/s NRZ-OOK at 40 kilometres is still open which suggests a possibility of deployment at longer distances. Closure of an eye diagram is mainly caused by Inter Symbol Interference (ISI), which occurs due to chromatic dispersion.

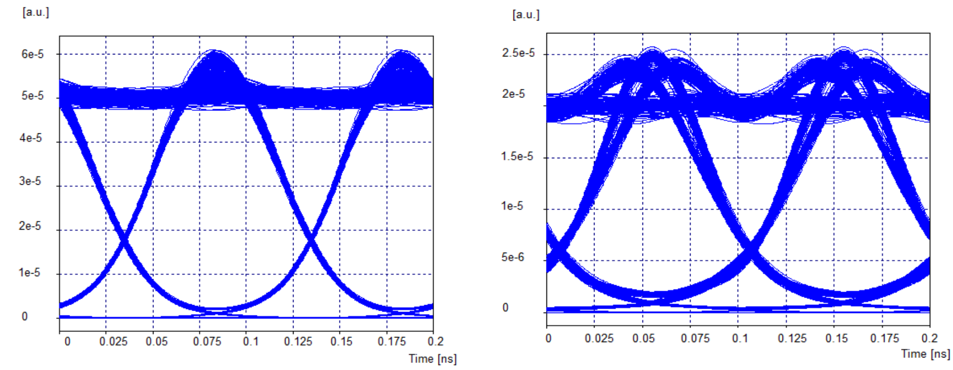

(a) : Eye diagram at 20 kilometres, BER $= 1 \cdot 10^{-40}$

(b) : Eye diagram at 40 kilometres, BER $= 3.3115 \cdot 10^{-19}$

Figure 4.11: Eye diagrams of 10 Gbit/s NRZ-OOK system at various fibre lengths

Since the chromatic dispersion tolerance of 20 Gbit/s NRZ-DPSK is a lot lower, ISI heavily impacts signal quality at far shorter distances in comparison with 10 Gbit/s NRZ-OOK. As a result, eye diagram closes already at 22 kilometres. In addition, signal quality deteriorates much faster than in the case of 10 Gbit/s NRZ-OOK. BER at 15 kilometres is still equal to $1 \cdot 10^{-40}$, however already at 22 kilometres is equal to $0.26319 \cdot 10^{-7}$. Eye diagrams for 20 Gbit/s NRZ-DPSK at various fibre lengths are shown in figure 4.12.

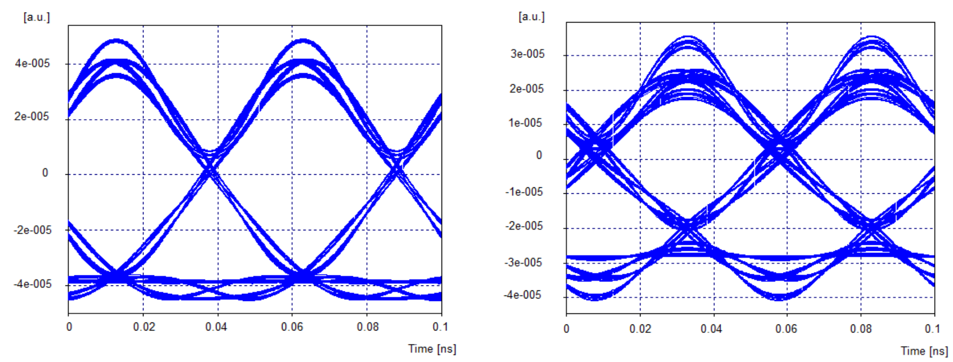

(a) : Eye diagram at 15 kilometres, BER $= 1 \cdot 10^{-40}$

(b) : Eye diagram at 22 kilometres, BER $= 3.6345 \cdot 10^{-8}$

Figure 4.12: Eye diagrams of 20 Gbit/s NRZ-DPSK system at various fibre lengths

In case of 40 Gbit/s NRZ-DQPSK signal distortion is already apparent in the order of kilometres, when BER threshold is exceeded at 10 kilometres. Due to higher bitrate this modulation format suffers from ISI even more than 20 Gbit/s NRZ-DPSK, which results in very sharp increase in BER starting already at 4 kilometres. Eye diagrams for 40 Gbit/s NRZ-DQPSK at various fibre lengths are shown in figure 4.13.

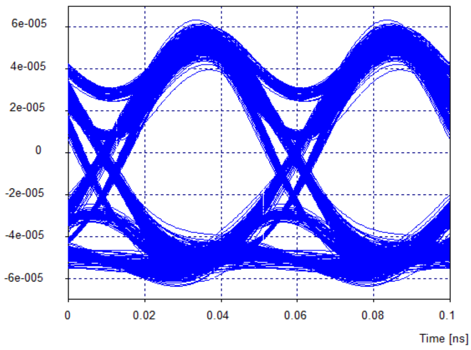

(a) : Eye diagram at 4 kilometres, BER $= 1 \cdot 10^{-40}$

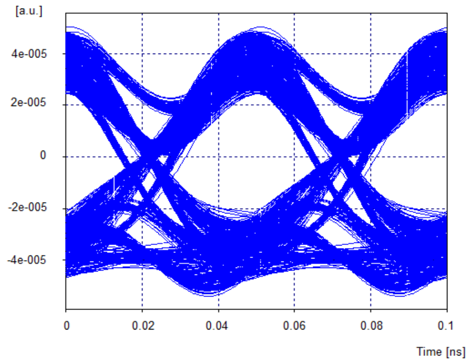

(b) : Eye diagram at 10 kilometres, BER $= 8.5210 \cdot 10^{-9}$

Figure 4.13: Eye diagrams of 40 Gbit/s NRZ-DQPSK system at various fibre lengths

In the second scenario I examined coexistence of previously utilised modulation formats in WDM-PON network. This scenario corresponds to the situation, when network operator wants to allocate higher bitrate wavelengths to premium customers while coexisting with ordinary line rate. Simulated WDM-PON netowrk is made up of 8 Optical Network Units (ONUs) and 8 Optical Line Termination (OLT) modules with dedicated wavelengths for downstream and upstream. This setup corresponds to 16 channels. Spectrum of channels comprises two 40 Gbit/s NRZ-DQPSK channels, four 40 Gbit/s NRZ-DPSK channels and ten 10 Gbit/s NRZ-OOK channels. Detailed channel distribution depicts figure, where group A corresponds to 10 Gbit/s NRZ-OOK channels, group B corresponds to 20 Gbit/s NRZ-DPSK channels and group C corresponds to 40 Gbit/s NRZ-DQPSK channels. Similarly to the previously simulated layout, maximal fibre length was set at 40 kilometres, launch power level was equal to 0 dBm and channel spacing was equal 100 GHz. Simulation layout does not include any regeneration segments, where signal recovery is performed. Figure 4.15 shows dependence of BER and Q-factor on fibre length for coexisting modulation formats.

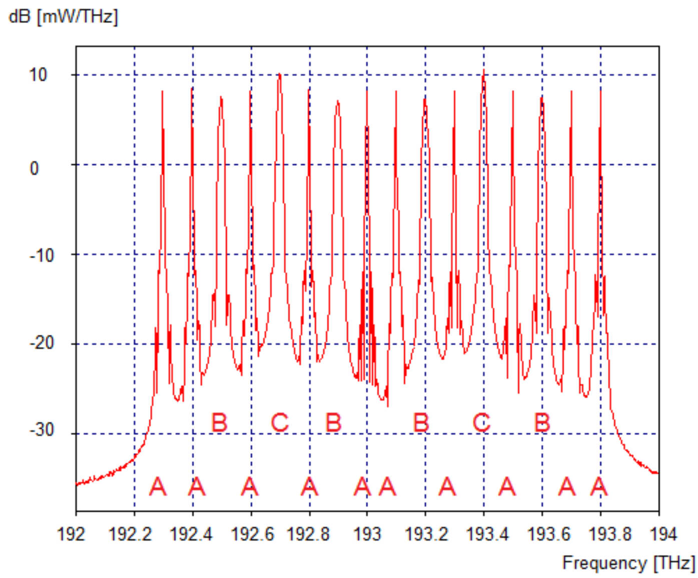

Figure 4.14: Channel distribution in the WDM-PON network with different modulation formats

Comparing figure 4.10 and figure 4.15 one can see that there is only a negligible difference in BER and Q-factor values between separate and coexisting systems. In case of 40 Gbit/s NRZ-DQPSK channels, maximal fibre length for quality transmission is around 9 kilometres, whereas in case of 20 Gbit/s NRZ-DPSK maximal fibre length increases to 20 kilometres. As well as in the previous simulation setup, 10 Gbit/s NRZ-OOK showed the best results, while not exceeding BER threshold even at 40 kilometres. Based on that it can be concluded that coexistence of these modulation formats do not pose a problem under the simulation conditions set in this simulation layout, as the resulting BER and Q-factor values do not significantly differ. This cannot, however, be regarded as a general truth, as different conclusions can be drawn with regard to different simulation conditions, such as channel spacing or launch power level.

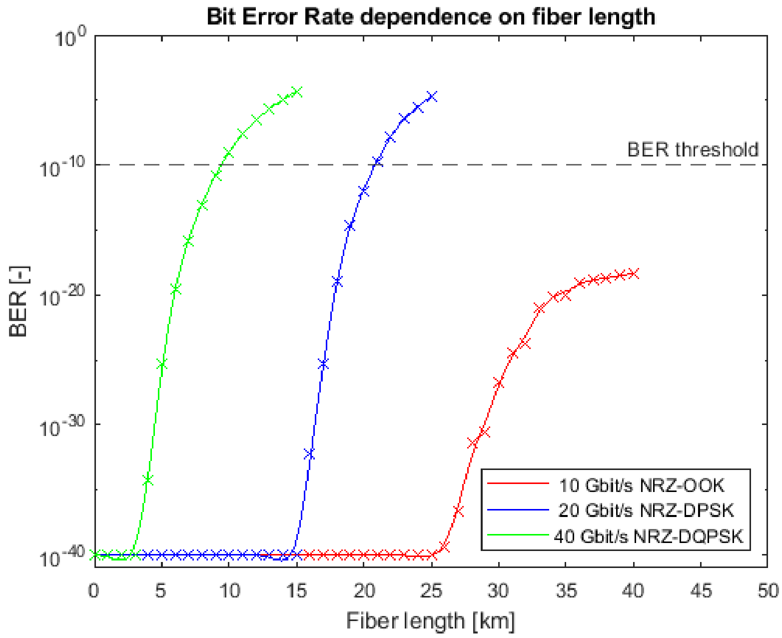

(a) : BER vs fibre length

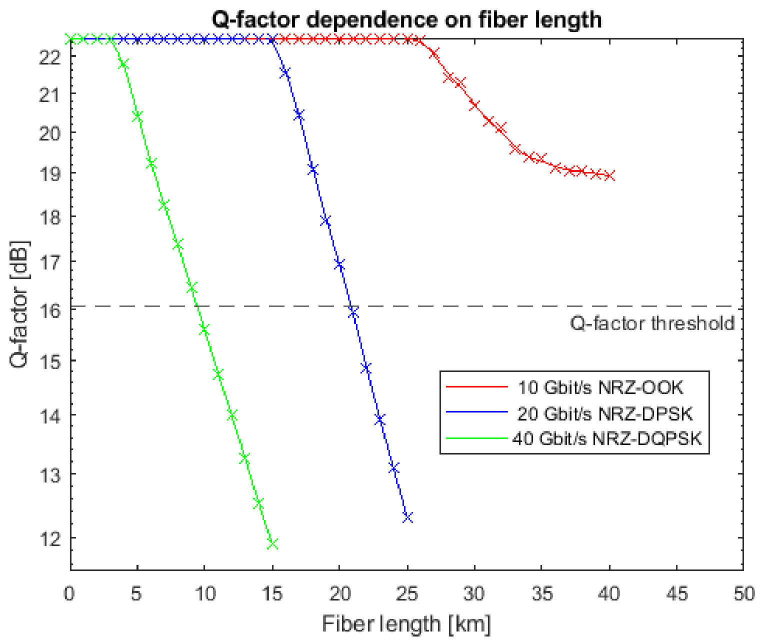

(b) : Q-factor vs fibre length

Figure 4.15: Signal degradation dependence on fibre length in case of coexisting modulation formats in PON setup

4.3 Influence of launch power level on the DWDM system

In this section, influence of launch power level on the DWDM system, where multiple modulation formats coexist, was examined. DWDM system consists of 15 channels on the 100 GHz grid. Signal was regenerated in the repeated segments deployed in the section 4.1, where fibre attenuation and chromatic dispersion were compensated. Channel distribution corresponds to the previously mentioned coexistence of DQPSK/DPSK/OOK modulation formats. Odd channels correspond to 10 Gbit/s NRZ-OOK channels (group A) and even channels are split into 2 alternating groups (group B and group C). Group B corresponds to the 20 Gbit/s NRZ-DPSK channels and group C corresponds to the 40 Gbit/s NRZ-DQPSK channels. In this simulation setup, launch power level was swept between -5 dBm and 10 dBm, while regeneration interval was fixed at 50 km. I decided to fix regeneration interval at 50 km, because on the basis of the previous results, see figure 4.9, all modulation formats showed the best performance at this interval, which enabled me to observe the impact of launch power level a lot better in comparison with longer regeneration interval, where BER was too high. The aim of this simulation was to investigate the effect of launch power level on BER and Q-factor. It could be assumed that there should be an optimal value of launch power level, for which BER and Q-factor reach their lowest and highest value, respectively. Dependence of BER and Q-factor on launch power level is shown in figure 4.16.

By observing graph 4.16 one can notice that there is a common optimal value of launch power level for all modulation formats, namely 2 dBm. When the launch power level is lower than this optimal value, there is a rise in BER. This is caused by lower OSNR, as optical signal with lower launch power level is transmitted. On the other hand, when optical signal with higher launch power level than the optimal value is transmitted, BER starts to increase as well. This is due to nonlinear effects, which are gradually becoming more dominant and therefore deteriorate the signal quality. By and large, launch power level plays an important role in the optical system design and an optimal value, when nonlinear effects are not dominant and the launch power level is not too low, must be found.

Further, one can see that NRZ-DPSK showed the best performance among deployed modulation formats regardless of the launch power level values. NRZ-DQPSK was quite stable showing slow decline, as the launch power level was swept. In case of NRZ-DQPSK BER threshold was exceeded only at 10 dBm. The worst performance was showed by 10 Gbit/s NRZ-OOK, which exceeded BER threshold at -4 dBm and 9 dBm.

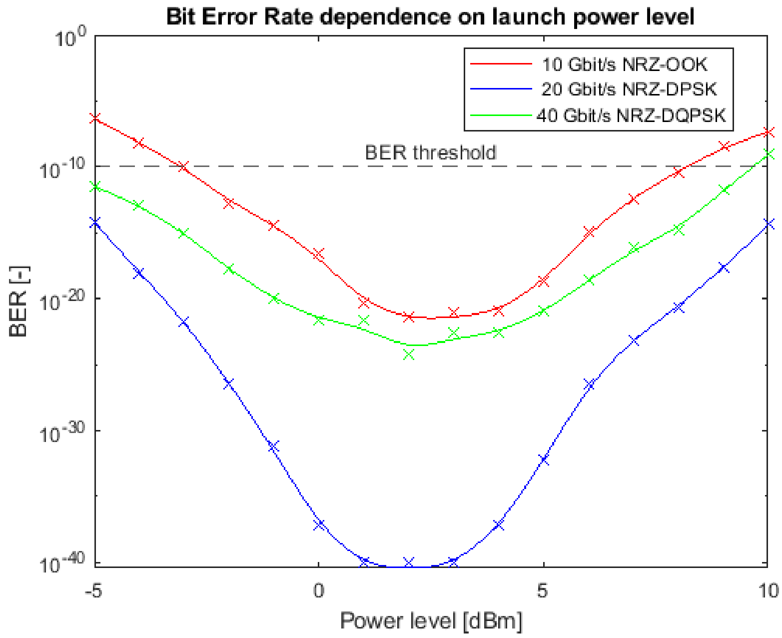

(a) : BER vs launch power level

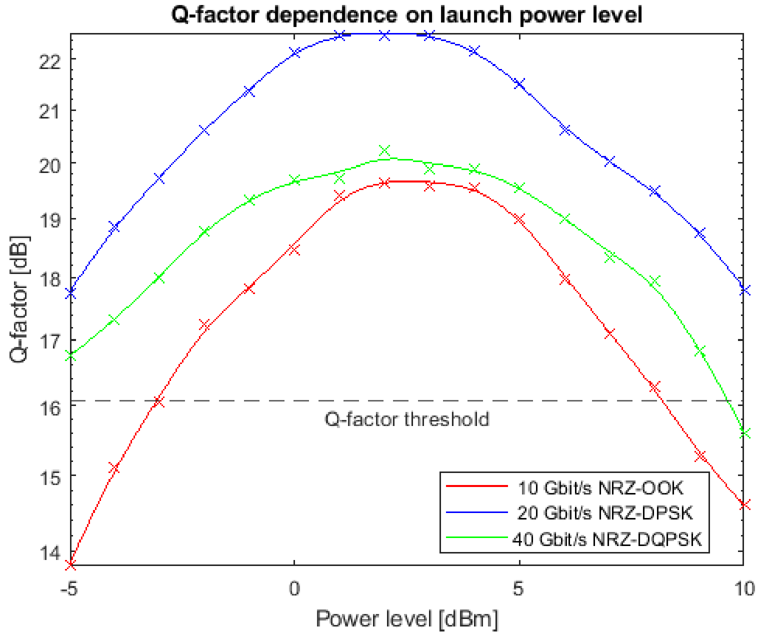

(b) : Q-factor vs launch power level

Figure 4.16: BER and Q-factor dependence on launch power level in case of coexistence of NRZ-OOK, NRZ-DPSK and NRZ-DQPSK

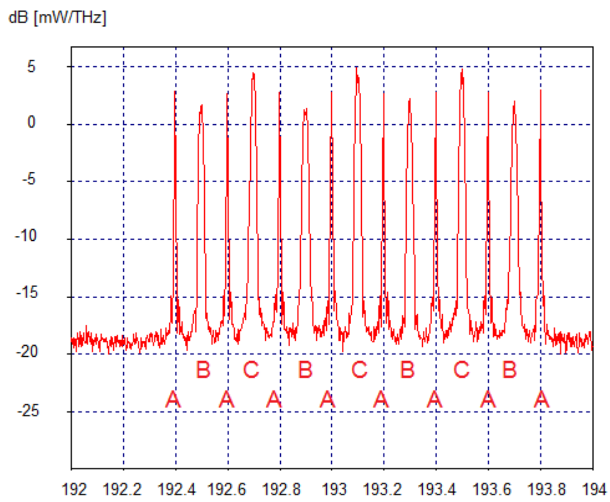

Figure 4.17: Output spectrum of DQPSK/DPSK/OOK system, launch power level $= -5$ dBm

In the figure 4.17 one can see the output spectrum of the analysed DQPSK/DPSK/OOK system with launch power level equal to -5 dBm. Although channels do not suffer from nonlinear effects, BER and Q-factor values are not the optimal ones, since OSNR is decreased due to lower launch power level , which corresponds to the attenuation of 25 kilometres long fibre in comparison with 0 dBm launch power level.

When the launch power level is increased to 2 dBm, the optimal value of BER and Q-factor will be reached. However, already at this launch power level one can observe new frequency components emerging in the output spectrum, see figure 4.18. These frequency components emerge very close to the original frequency components. Nevertheless, their influence on the original channels is negligible at this launch power level.

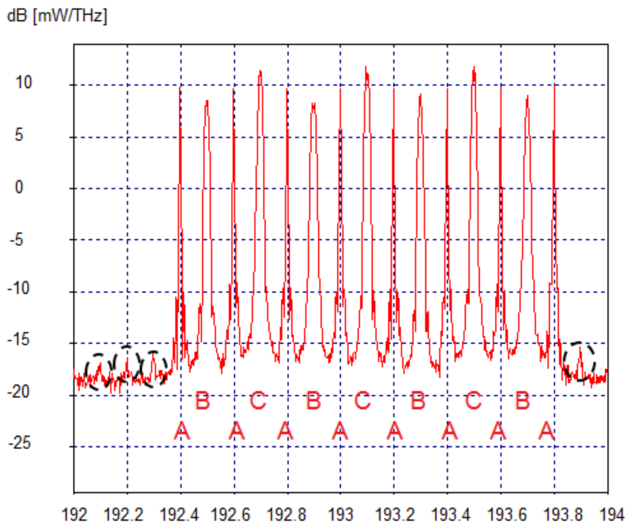

Figure 4.18: Output spectrum of DQPSK/DPSK/OOK system, launch power level = 2 dBm

Last simulated launch power level was equal to 10 dBm. At this launch power level, signal is severely deteriorated due to nonlinear effects and emergence of new frequency components, which are becoming significant in the output spectrum, see figure 4.19. Original frequency components suffer, as a result, from crosstalks from new frequency components, which emerge very close to the original channels.

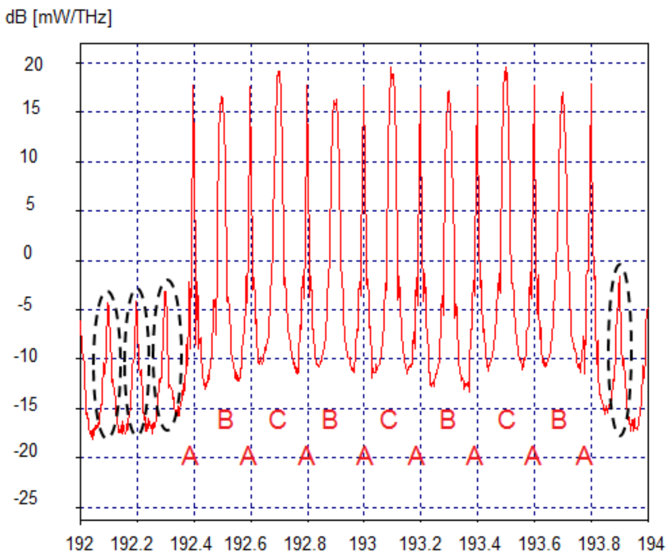

Figure 4.19: Output spectrum of DQPSK/DPSK/OOK system, launch power level = 10 dBm

4.4 Impact of channel spacing on the transmission quality

4.4.1 Individual modulation formats

I have so far investigated performance of DWDM system with three different modulation formats under various conditions, namely with variable regeneration interval, power level or fibre length without compensating elements. In this section I decided to follow up the first simulation setup, in which dependence of transmission quality on regeneration interval with fixed channel spacing is examined. In this simulation setup, channel spacing was set at 100 GHz, which corresponds to the ITU-T G.694.1 recommendation, see subsection 2.1.2. This recommendation defines 4 types of channel width, namely 100 GHz, 50 GHz, 25 GHz and 12,5 GHz. As a result, dependence of the transmission quality on regeneration interval in DWDM system with 3 modulation formats was investigated, while channel spacing parameter was set at the recommended value. DWDM systems with corresponding channel spacing were simulated at first separately with 1 modulation format deployed an then in the coexisting layout. Simulated DWDM system consists of 15 channels on the fixed frequency grid. launch power level is equal to 0 dBm. Signal is regenerated in the repeated segments, which comprise EDFA and FBG in post compensation setup. The aim of this simulation was to observe the impact of channel spacing on the transmission quality of each modulation format in DWDM system. Before I carried out the simulation, I conducted a parameter scan to find an optimal value of bandwidth of an optical band pass filter for each modulation format and each channel spacing. This value was then implemented in the simulation layout.

The first simulation setup examined the performance of individual modulation formats with 15 channels on the fixed frequency grid. Dependence of transmission quality on regeneration interval with channel spacing equal to 50 GHz depicts figure 4.20. Comparing figure 4.20 with figure 4.3 one can observe that reduction in channel spacing by factor of 2 does not bring about a significant degradation of transmission quality. Channels with 20 Gbit/s NRZ-DPSK even show improvement in transmission quality. The measured BER and Q-factor values are, however, only by few orders better, which I attribute to the simulation inaccuracy since basically the same results are obtained as in the case of 100 GHz channel spacing. This is, nevertheless, a positive outcome of this simulation for the network provider, because they can afford to double the number of channels with no deterioration in transmission quality, while occupying the same bandwidth.

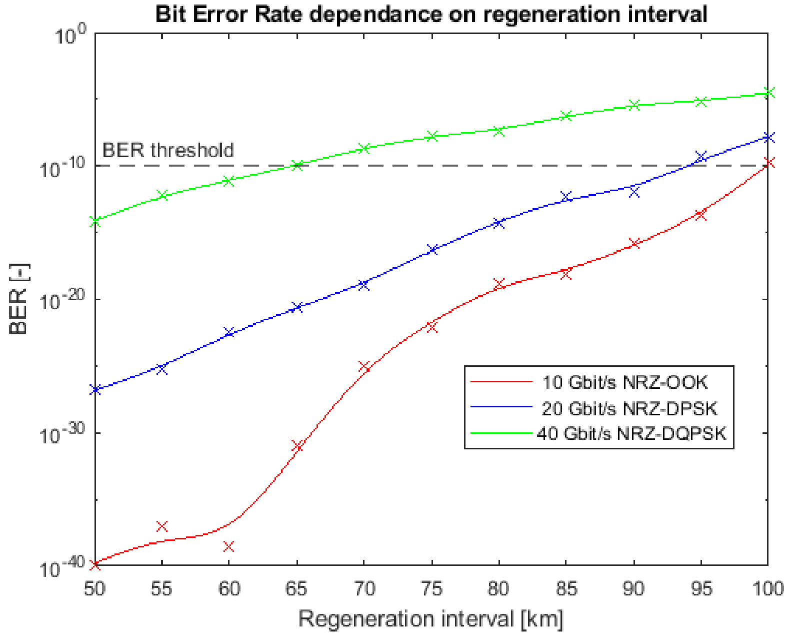

(a) : BER vs regeneration interval

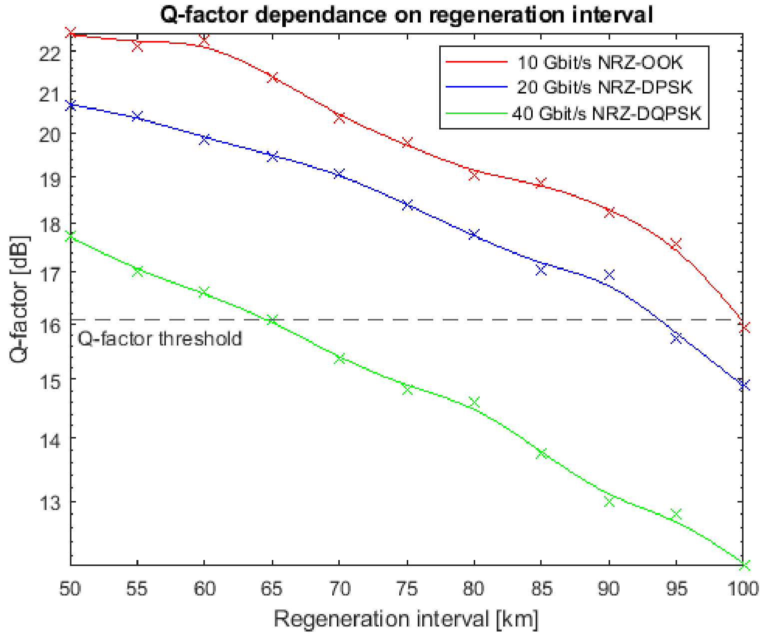

(b) : Q-factor vs regeneration interval

Figure 4.20: BER and Q-factor dependence on regeneration interval in case of separate systems with channel spacing equal to 50 GHz

The next simulation setup is identical to the previous one, but channel spacing was set at 25 GHz. Each DWDM system was as well as in the previous case tested separately and resulting BER and Q-factor values were plotted in a graph, which is depicted in figure 4.21. Looking at the graphs it is possible to observe that 40 Gbit/s NRZ-DQPSK channels are completely degraded with BER and Q-factor values equal to the worst possible values that could be obtained in the simulation. Moving to another modulation format, 20 Gbit/s NRZ-DPSK does not show a lot better results, when BER and Q-factor threshold is exceeded at all simulated regeneration interval lengths. As far as 10 Gbit/s NRZ-OOK channels are concerned, they performed very well while not exceeding BER and Q-factor threshold at any regeneration interval lengths. This clearly suggests that spectrum of 40 Gbit/s NRZ-DQPSK and 20 Gbit/s NRZ-DPSK is too wide to be operated on the 25 GHz grid in the separate DWDM setup. Conversely, 10 Gbit/s NRZ-OOK channels could be deployed on the 25 GHz grid with good transmission quality, which enables to have 4 times more channels while occupying the same bandwidth in comparison with 100 GHz channel grid. I decided not to carry out simulation of DWDM system with channel spacing equal to 12,5 GHz, since 20 Gbit/s NRZ-DPSK and 40 Gbit/s NRZ-DQPSK are already well below BER and Q-factor threshold.

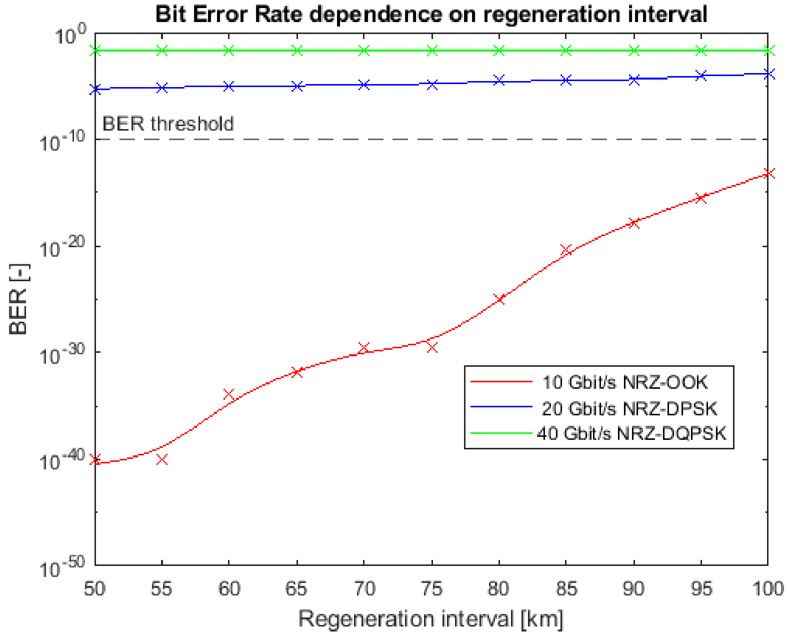

(a) : BER vs regeneration interval

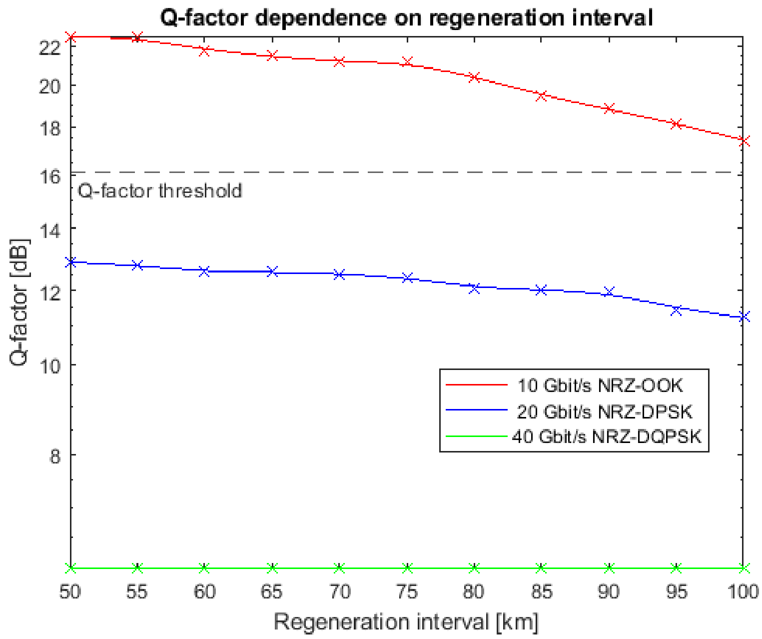

(b) : Q-factor vs regeneration interval

Figure 4.21: BER and Q-factor dependence on regeneration interval in case of separate systems with channel spacing equal to 25 GHz

4.4.2 Coexistence of modulation formats

In this subsection, all studied modulation formats were deployed in the DWDM system in the coexisting scenario. DWDM system is made up of 15 channels, launch power level is equal to 0 dBm. Signal is regenerated in the repeated segments consisting of EDFA and FBG in post compensation setup. Channel distribution is organised in the following way. Odd channels correspond to 10 Gbit/s NRZ-OOK and even channels correspond to 20 Gbit/s NRZ-DPSK alternating with 40 Gbit/s NRZ-DQPSK. Figure 4.22 shows channel distribution of DWDM system on 50 GHz grid. Dependence of BER and Q-factor on the regeneration interval in case of coexistence of different modulation format with channel spacing equal to 50 GHz is shown in figure 4.23.

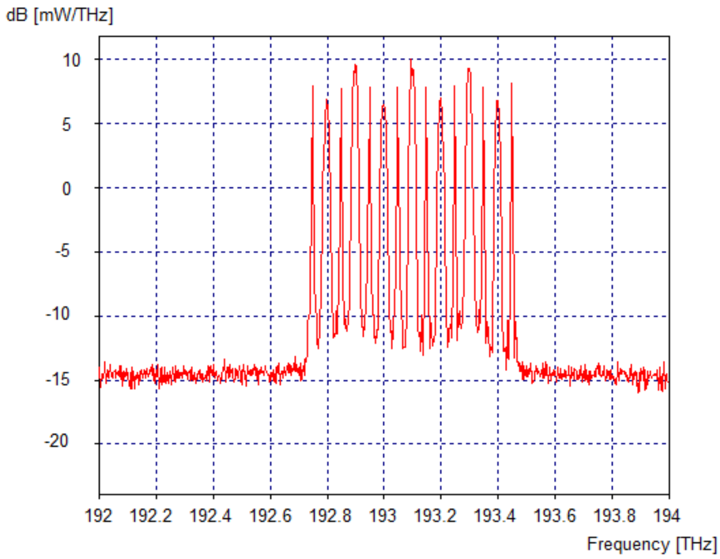

Figure 4.22: Output spectrum of DQPSK/DPSK/OOK system with channel spacing equal to 50 GHz

Comparing figure 4.23 with figure 4.9 one can observe only a slight difference in BER and Q-factor. All modulation formats show very similar performance to the simulation setup with 100 GHz grid. The worst performance was shown by 10 Gbit/s NRZ-OOK, which suffers from crosstalk from adjacent channels corresponding to 20 Gbit/s NRZ-DPSK and 40 Gbit/s NRZ-DQPSK. These modulation formats benefit from narrower spectrum of adjacent 10 Gbit/s NRZ-OOK channels, which result in better BER and Q-factor values. These results enable a network provider to better exploit the bandwidth, since one could halve the channel spacing without a significant deterioration of transmission quality comparing 100 GHz channel spacing and 50 GHz channel spacing

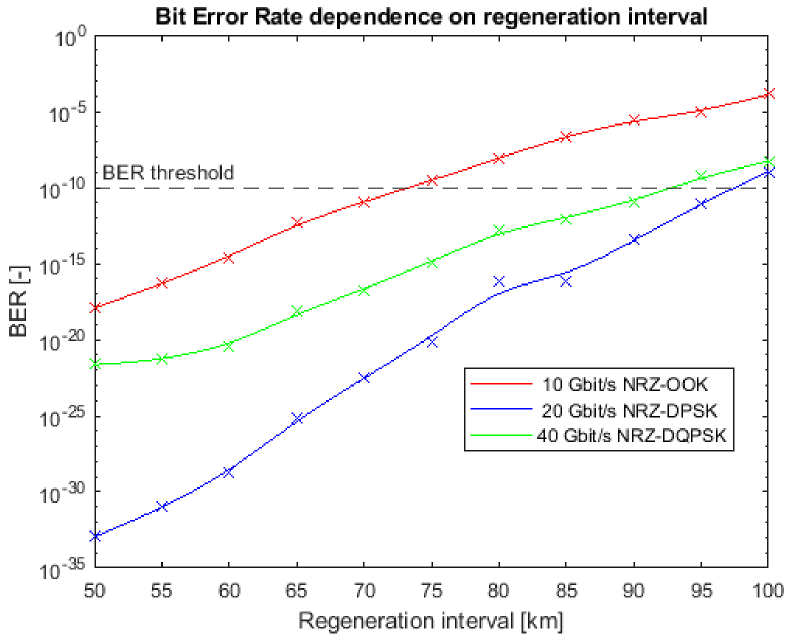

(a) : BER vs regeneration interval

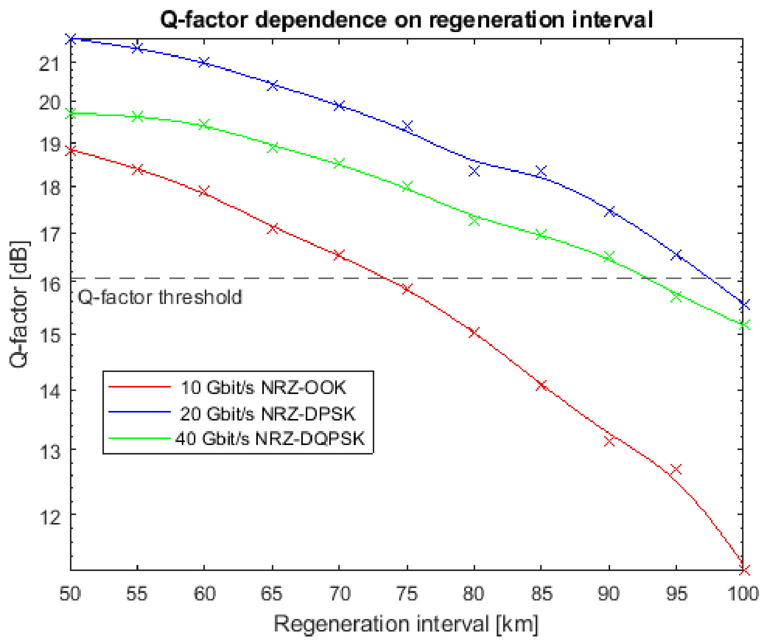

(b) : Q-factor vs regeneration interval

Figure 4.23: BER and Q-factor dependence on regeneration interval in case of coexistence of NRZ-OOK, NRZ-DPSK and NRZ-DQPSK with channel spacing equal to 50 GHz

In the next simulation, simulation conditions remain the same as in the previous case. DWDM system comprises 15 channels, launch power level is equal to 0 dBm. Signal is regenerated in the repeated segments consisting of EDFA and FBG in post compensation setup. Channel spacing is equal to 25 GHz, which is the only difference between the previous simulation layout and this one. Channel distribution remains the same as well. Odd channels correspond to 10 Gbit/s NRZ-OOK and even channels correspond to 20 Gbit/s NRZ-DPSK alternating with 40 Gbit/s NRZ-DQPSK. Channel distribution of DWDM system on 25 GHz grid illustrates figure 4.24. Dependence of BER and Q-factor on the regeneration interval in case of coexistence of different modulation format with channel spacing equal to 25 GHz is shown in figure 4.25.

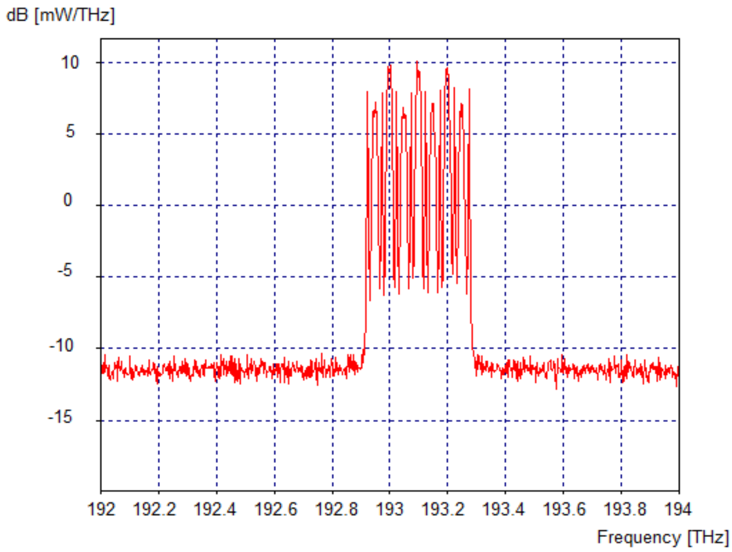

Figure 4.24: Output spectrum of DQPSK/DPSK/OOK system with channel spacing equal to 25 GHz

By observing figure 4.21 one can conclude that another reduction in the channel spacing by a factor of 2 has a big impact on the transmission quality of 10 Gbit/s NRZ-OOK channels. BER and Q-factor values obtained in the simulation are the lowest possible which suggests complete deterioration of transmission quality. This is caused by the spectrum width of adjacent channels corresponding to 20 Gbit/s NRZ-DPSK and 40 Gbit/s NRZ-DQPSK channels. Conversely, the other two modulation formats are also more affected by crosstalks in comparison with 50 GHz channel spacing, since adjacent 10 Gbit/s NRZ-OOK channels are also closer to them, and thus affect them.

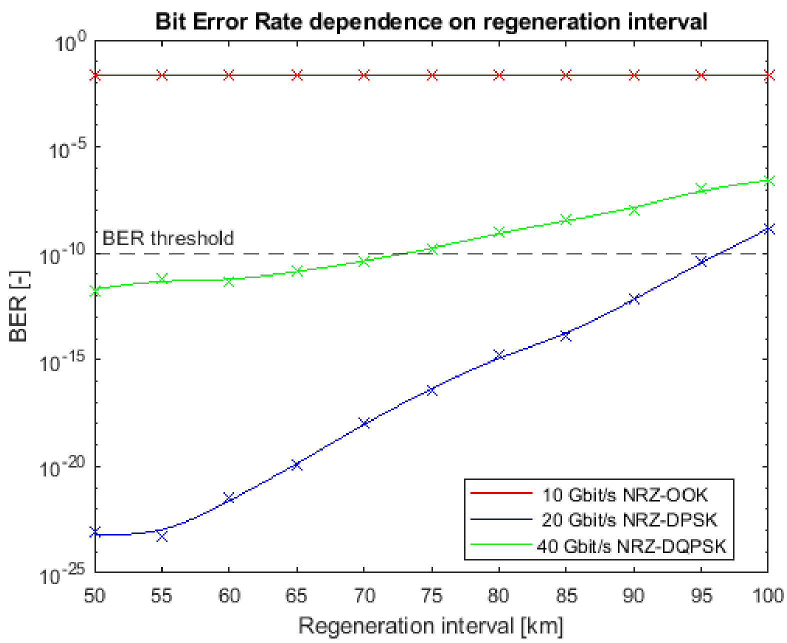

(a) : BER vs regeneration interval

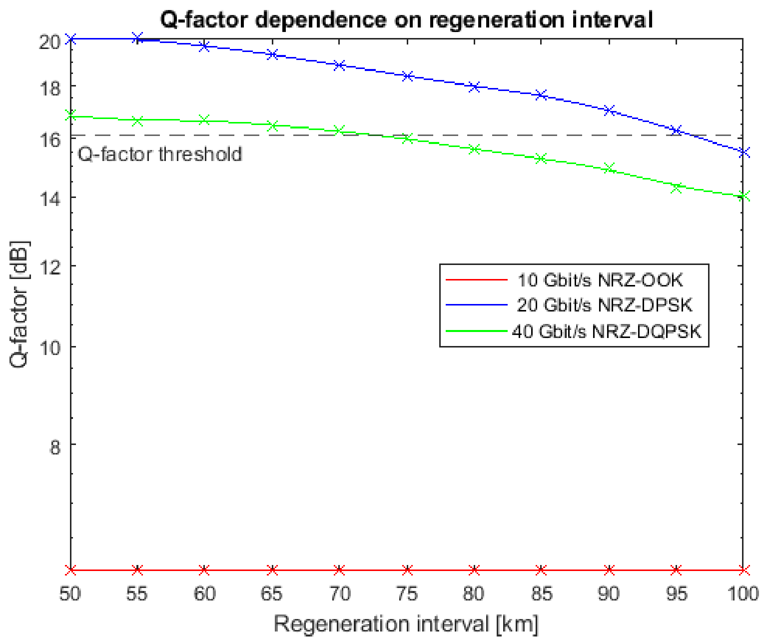

(b) : Q-factor vs regeneration interval

Figure 4.25: BER and Q-factor dependence on regeneration interval in case of coexistence of NRZ-OOK, NRZ-DPSK and NRZ-DQPSK with channel spacing equal to 25 GHz

4.5 Coexistence of PM-NRZ-QPSK and NRZ-OOK channels on the 50 GHz grid

As the capacity of the legacy 10 Gbit/s NRZ-OOK DWDM systems is becoming insufficient, more spectrally efficient modulation formats are being developed. One of them is definitely PM-QPSK modulation format, which is expected to provide a solution for implementing 100 Gbit/s per wavelength while coexisting with existing NRZ-OOK systems. This is, however, at the cost of complexity of the receiver, although use of signal digital processing can dramatically simplify the receiver design, which is covered in subsection 2.5.4.

In this subsection, I carried out a simulation, where one 100 Gbit/s PM-QPSK channel (PM-QPSK signal is generated from four 26.75 Gbit/s data channels, as overhead is included for forward error correction) coexists with eight 10 Gbit/s NRZ-OOK channels in DWDM system on 50 GHz grid. Channels were distributed in such a way that central PM-QPSK channel was surrounded by four 10 Gbit/s NRZ-OOK channels on either side. Signal was regenerated in the repeated segments deployed in the previous simulation layouts. However, repeated segments did not comprise Fibre Bragg Grating for chromatic dispersion compensation, as PM-QPSK receiver already consists of Electronic Dispersion Compensator. Nevertheless, in case of 10 Gbit/s NRZ-OOK channels Fibre Bragg Grating was used before signal demultiplexing to compensate for chromatic dispersion. There were 8 repeated segments with fibre length equal to 50 kilometres making 400 kilometres long optical link. Loss of the optical fibre was fully compensated by EDFA in the repeated segments. The aim of this simulation was to examine the influence of launch power level of 10 Gbit/s NRZ-OOK channels on the transmission quality of both modulaion formats with launch power level of PM-QPSK as a parameter. Unlike previous simulation layouts, in case of PM-QPSK modulation format, different method of BER evaluation is used. In this case, direct counting of error bits is implemented using Viterbi-Viterbi algorithm [64]. As a result, to establish a bit error rate of 10^{-12} by direct counting of errors would require the simulation of trillions of bits, which is totally out of question. Consequently, total number of simulated bits were 65 536 which enabled to obtain pre-FEC values in the order of 10^{-3}, while 1 run duration was still reasonably short (tens of minutes). If the number of error bits was equal to zero, the nearest positive integer was recorded instead, since zero error bits cannot be plotted in the logarithmic scale. Dependence of BER on the launch power level of 10 Gbit/s NRZ-OOK channels is shown in figure 4.26.

Looking at the graph it is possible to see that in both cases BER dramatically increases, when certain value of launch power level is exceeded. This is due to nonlinear effects which start to dominate at 8 dBm and higher power levels, as new frequency components emerge very close to the original channels due to FWM.

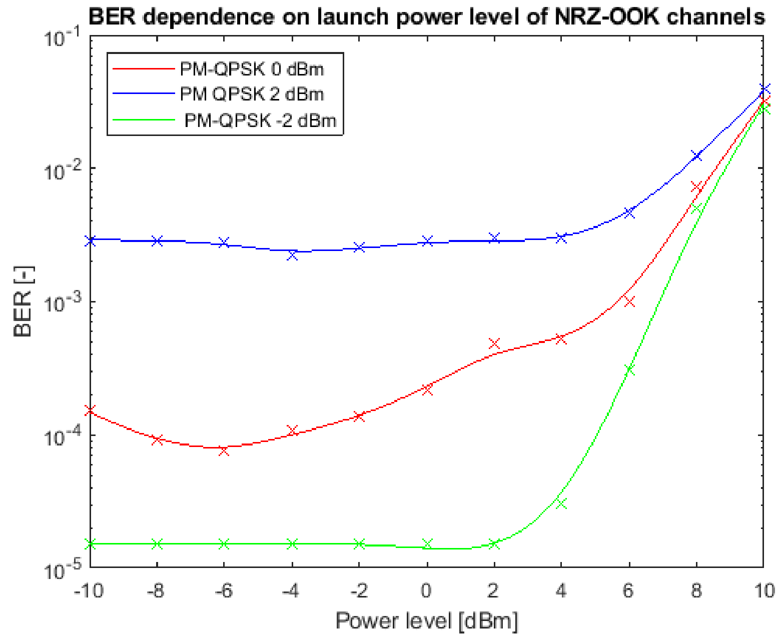

(a) : BER of PM-QPSK channels vs launch power level of 10 Gbit/s NRZ-OOK channels

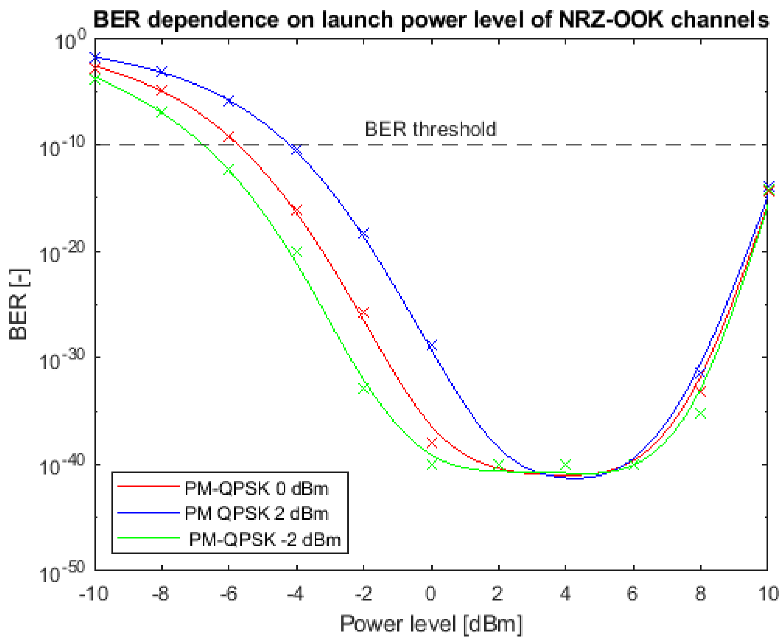

(b) : BER of 10 Gbit/s NRZ-OOK channels vs launch power level of 10 Gbit/s NRZ-OOK channels

Figure 4.26: BER dependence on launch power level in case of coexistence of PM-QPSK and NRZ-OOK

BER of 10 Gbit/s NRZ-OOK channels has its optimum between 2 and 6 dBm, while lower values of power level negatively impact BER of NRZ-OOK channels, as lower OSNR and crosstalks from PM-QPSK channel deteriorate transmission quality. BER of PM-QPSK channel does not dramatically change with launch power level of OOK channels lower than 2 dBm. Further, one can observe the effect of launch power level of PM-QPSK channel. The best transmission quality in both cases is reached with launch power level of PM-QPSK equal to -2 dBm. Th higher the launch power level of PM-QPSK channel is, the worse BER values are obtained regardless of the modulation format. This is probably due to stronger crosstalks and nonlinear effects, which are more dominant with higher power levels. By and large, a network provider must take into account that coexistence of these modulation formats is viable and works, but if the launch power level is not adequately set, both formats can negatively affect themselves, resulting in BER increase.

Chapter 5

Conclusion

This thesis aimed to study potential coexistence of multiple optical systems at the physical layer for different implementation options and network load, while providing models of coexistence of different transmission systems based on the computer simulations in Optsim environment. The results indicate that coexistence of multiple optical systems is viable, although limitations of this approach must be taken into account.

It was demonstrated that transmission quality clearly benefits from shorter regeneration interval, even though more regeneration segments introduce more noise into the system.

Further, the impact of coexistence of modulation formats with different line rate was investigated. The simulation results show that legacy 10 Gbit/s NRZ-OOK is largely affected by adjacent 20 Gbit/s NRZ-DPSK and 40 Gbit/s NRZ-DQPSK channels, leading to shorter regeneration interval required to meet transmission quality requirements in comparison with legacy 10 Gbit/s NRZ-OOK DWDM system.

Furthermore, performance of utilised modulation formats was investigated in the PON scenario. In this case 10 Gbit/s NRZ-OOK demonstrated its superiority over 20 Gbit/s NRZ-DPSK and 40 Gbit/s NRZ-DQPSK as far as short optical links are concerned. In addition, simulation results showed that coexistence of these modulation formats in the PON scenario did not bring about significant deterioration in transmission quality.

Impact of channels spacing on the transmission quality was also elaborated. Simulation results revealed that transition from 100 GHz grid to 50 GHz grid hat little impact on the transmission quality in both separate systems scenario and coexistence scenario. However, another shift towards shorter channel spacing proved to be a problem. In case of separate DWDM systems, both 20 Gbit/s NRZ-DPSK and 40 Gbit/s NRZ-DQPSK cannot be operated on this frequency grid, as the frequency spectrum of these modulation formats is too wide. As far as coexisting modulation formats are concerned, 10 Gbit/s NRZ-OOK channels were severely damaged by adjacent 20 Gbit/s NRZ-DPSK and 40 Gbit/s NRZ-DQPSK channels, showing the highest possible BER that could be obtained in Optsim environment.

Influence of launch power level on coexisting 40 Gbit/s NRZ-QDPSK, 20 Gbit/s NRZ-DPSK and 10 Gbit/s NRZ-OOK modulation formats was also explored. It was demonstrated that 20 Gbit/s NRZ-DPSK showed the best performance regardless of the launch power level. In addition, it was shown that certain optimal value of launch power level had to be found in order to obtain the best possible BER and Q-factor values. This is also true of coexistence of 100 Gbit/s PM-QPSK with surrounding legacy 10 Gbit/s NRZ-OOK channels. It was proved that launch power level of 10 Gbit/s NRZ-OOK was crucial to the overall transmission quality and had to be optimized to minimize undesirable nonlinear effects affecting both modulation formats.

Considering the presented results, the main objectives of this thesis were met. One of the main contributions presented in this thesis are models of coexistence and their parametrization, as influence of various system parameters, such as channel spacing, launch power level, line rate or modulation format, was extensively elaborated.

The possible limitations could be inherent inaccuracy, as the number of simulated bits was limited, especially in case of coexistence of PM-QPSK and NRZ-OOK, when direct error counting was applied in the PM-QPSK receiver. Another limiting factor could be the closed-source nature of Optsim environment as experimental measurements could potentially verify obtained results.

Future studies may build on this thesis, as a number of aspects were touched upon briefly or not at all, for example more advanced modulation formats with line rates higher than 100 Gbit/s, ultra long-haul fibre links, as this thesis dealt with 400 km long fibre link, or nonlinear effects emerging at high power levels, such as Stimulated Raman Scattering or Stimulated Brillouin Scattering.

List of Abbreviations

ASE Amplified Spontaneous Emission. 11, 26

BER Bit Error Rate. 1, 2, 8, 10, 13, 22, 23, 26, 28, 33, 35, 37, 39–41, 43, 45, 48, 51, 53, 55, 57, 60

CWDM Course Wavelength Division Multiplex. 3, 4

DCF Dispersion Compensating Fibre. 7, 8

DQPSK Differential Quadrature Phase Shift Keying. 15

DWDM Denseavelength Division Multiplex. 3, 9–11

EDC Electronic Dispersion Compensation. 7

EDFA Erbium Doped Fibre Amplifier. 10, 11, 27, 28, 31, 51, 53

FBG Fibre Bragg Grating. 7, 31, 51, 53

FWM Four Wave Mixing. 9–11, 55

GFF Gain Flattening Filter. 12

ISI Inter Symbol Interference. 7, 12, 39, 40

MAN Metropolitan Area Network. 4

MLR Mixed Line Rates. 19

MZM Mach-Zehnder Modulator. 14

OPC Optical Phase Conjugator. 11

OSNR Optical Signal to Noise Ratio. 13, 16, 17, 43, 45

PDM Polarization Divison Multiplex. 16, 17

PLI Physical Layer Impairments. 1

PM Phase Modulator. 14

PMD Polarization Mode Dispersion. 8, 9, 12, 15, 17, 20, 26

PMF Polarization Maintaining Fibre. 8

SBS Stimulated Brillouin Scattering. 9

SMF Single Mode Fibre. 7, 8

SNR Signal to Noise Ratio. 9, 23

SPM Self-Phase Modulation. 9

SRS Stimulated Raman Scattering. 9, 21

TDSS Time Domain Split-step. 21

VCSEL Verticaly Cavity Surface Emitting Laser. 4

WDM Wavelength Division Multiplex. 3

XPM Cross-Phase Modulation. 9, 10, 16, 19, 20

Bibliography

[1] NAG, Avishek, Massimo TORNATORE and Biswanath MUKHERJEE. Energy-efficient and cost-efficient capacity upgrade in mixed-line-rate optical networks. *IEEE/OSA Journal of Optical Communications and Networking* [online]. December 2012, **4**(12), 1018 - 1025 [cit. 2021-04-12]. Available from: https://ieeexplore.ieee.org/abstract/document/6392506

[2] NAG, Avishek, Massimo TORNATORE and Biswanath MUKHERJEE. Optical Network Design With Mixed Line Rates and Multiple Modulation Formats. *Journal of Lightwave Technology* [online]. October 2009, **28**(4), 466 - 475 [cit. 2021-04-12]. Available from: https://ieeexplore.ieee.org/document/5286317

[3] NAG, Avishek and Massimo TORNATORE. Impact of channel spacing on the design of a mixed-line-rate optical network. *2009 IEEE 3rd International Symposium on Advanced Networks and Telecommunication Systems (ANTS)* [online]. December 2009 [cit. 2021-04-12]. Available from: https://ieeexplore.ieee.org/document/5409872

[4] UDALCOVS, Aleksejs, Paolo MONTI, Vjaceslavs BOBROVS, et al. Spectral and energy efficiency considerations in mixed-line rate WDM networks with signal quality guarantee. *2013 15th International Conference on Transparent Optical Networks (ICTON)* [online]. June 2013 [cit. 2021-04-12]. Available from: https://ieeexplore.ieee.org/document/6602845

[5] UDALCOVS, Aleksejs, Girts IVANOVS and Vjaceslavs BOBROVS. Comparison between power efficiencies of mixed-line rate over Single-Line Rate in spectral efficient WDM networks with signal quality guarantee. *2013 IEEE Latin-America Conference on Communications* [online]. November 2013 [cit. 2021-04-12]. Available from: https://ieeexplore.ieee.org/document/6759811

[6] VODRÁŽKA, Jiří and Pavel LAFATA. Optické přístupové sítě a přípojky FTTx. České vysoké učení technické v Praze: Nakladatelství ČVUT, 2014. ISBN 978-80-01-05463-5.

[7] The principle scheme of the WDM system. *ResearchGate* [online]. [cit. 2021-04-12]. Available from: https://www.researchgate.net/figure/The-principle-scheme-of-the-WDM-system_fig1_318258775

[8] fibre optics. *A2net.eu* [online]. [cit. 2021-04-12]. Available from: http://a2net.eu/fibreoptics.html

[9] CWDM or DWDM: Which Should You Use and When? *World Wide Technology* [online]. [cit. 2021-04-12]. Available from: https://www.wwt.com/article/cwdm-or-dwdm-which-should-you-use-and-when

[10] DWDM frequency grid with the flexible channel spacing. *ResearchGate* [online]. [cit. 2021-04-12]. Available from: https://www.researchgate.net/figure/The-DWDM-frequency-grid-with-the-flexible-channel-spacing-The-Simulation-Platform-for_fig3_333633719

[11] BOHÁČ, Leoš and Michal LUCKI. Optické komunikační systémy. Praha: Česká technika-nakladatelství ČVUT, 2010. ISBN 978-80-01-04484-1.

[12] BOBROVS, Vjaceslavs, Sandis SPOLITIS and Girts IVANOVS. Comparison of chromatic dispersion compensation techniques for WDM-PON solution. *2012 2nd Baltic Congress on Future Internet Communications* [online]. April 2012 [cit. 2021-04-12]. Available from: https://ieeexplore.ieee.org/document/6217981

[13] PATEL, Ankit V., R. B. PATEL and Kinjal A. MEHTA. Comparative analysis of single span high speed 40 Gbps long haul optical link using different modulation formats in the presence of Kerr nonlinearity. *Proceedings of the 2014 IEEE Students' Technology Symposium* [online]. March 2014 [cit. 2021-04-12]. Available from: https://ieeexplore.ieee.org/document/6217981

[14] BAJPAI, Rochak, Sujata SENGAR and Shree Prakash SINGH. Performance Comparison of 40 Gbps Mixed Line Rate WDM System for Various Dispersion Compensation Schemes. *2018 International Conference on Computational and Characterization Techniques in Engineering and Sciences (CCTES)* [online]. September 2018 [cit. 2021-04-12]. Available from: https://ieeexplore.ieee.org/document/8674103

[15] Polarization mode dispersion along birefringent fibre. *ResearchGate* [online]. [cit. 2020-11-03]. Available from: https://www.researchgate.net/figure/9-Polarization-mode-dispersion-along-birefringent-fibre-Adapted-from-65_fig10_315690740

[16] VRANOVA, Zuzana, Pavel CERNY, Lukas ROUDNY and Antonin MAZALEK. The Dispersion of Single-Mode Optical Fibres : How to Measure and Minimise it. *2019 International Conference on Military*

Technologies (ICMT) [online]. May 2019 [cit. 2021-04-12]. Available from: https://ieeexplore.ieee.org/document/8870049

[17] HASAN, Md. Rabiul, Md. Shamim ANOWER and Md. Imran HASAN. A Polarization Maintaining Single-Mode Photonic Crystal fibre for Residual Dispersion Compensation. *IEEE Photonics Technology Letters* [online]. May 2016, **28**(16) [cit. 2021-04-12]. Available from: https://ieeexplore.ieee.org/document/7478104

[18] JOHNSON, Sandra Brigit, P. Saranya NATH and Renju Thomas JACOB. Polarization mode dispersion reduction in optical fibres. *2014 International Conference on Green Computing Communication and Electrical Engineering (ICGCCEE)* [online]. March 2014 [cit. 2021-04-12]. Available from: https://ieeexplore.ieee.org/document/6922227

[19] VYUKUSENGE, A. and J. RABENANDRASANA. Polarization Mode Dispersion Effects on Signal Quality and Compensation Methods. *2020 Systems of Signals Generating and Processing in the Field of on Board Communications* [online]. March 2020 [cit. 2021-04-12]. Available from: https://ieeexplore.ieee.org/document/9078548

[20] RUZBARSKY, Jan, Jan TURAN and Lubos OVSENIK. Stimulated Brillouin scattering in DWDM all optical communication systems. *2016 26th International Conference Radioelektronika (RADIOELEKTRONIKA)* [online]. April 2016 [cit. 2021-04-12]. Available from: https://ieeexplore.ieee.org/document/7477354

[21] ROMANOV, O. I., M. V. ORYSCHUK and Y. S. HORDASHNYK. Computing of influence of stimulated Raman scattering in DWDM telecommunication systems. *2016 International Conference Radio Electronics and Info Communications (UkrMiCo)* [online]. September 2016 [cit. 2021-04-12]. Available from: https://ieeexplore.ieee.org/document/7739622

[22] SABAPATHI, T. and R. POOVITHA. Combating the effect of nonlinearities in DWDM system. *2017 4th International Conference on Electronics and Communication Systems (ICECS)* [online]. February 2017 [cit. 2021-04-12]. Available from: https://ieeexplore.ieee.org/document/8067876

[23] RASHEED, Iftikhar, Muhammad ABDULLAH, Shahid MEHMOOD and Mahwish CHAUDHARY. Analyzing the non-linear effects at various power levels and channel counts on the performance of DWDM based optical fibre communication system. *2012 International Conference on Emerging Technologies* [online]. October 2012 [cit. 2021-04-12]. Available from: https://ieeexplore.ieee.org/document/6375446

[24] TAHER, Kazi Afsara, Rafid Ur RAHMAN, Raina IFTEKHAR, et al. Effect of Cross Phase Modulation in Wavelength Division Multiplexing Optical System with EDFA. *2019 IEEE International Conference on Telecommunications and Photonics (ICTP)* [online]. December 2019 [cit. 2021-04-12]. Available from: https://ieeexplore.ieee.org/document/9041823

[25] Four-Wave Mixing (FWM). *Understanding Optical Communications:Optical Fibre* [online]. [cit. 2020-11-10]. Available from: https://imedea.uib-csic.es/~salvador/docencia/coms_optiques/addicional/ibm/ch02/02-19.html

[26] MAHARJAN, Rupendra, Ingrida LAVRINOVICA, Andis SUPE and Jurgis PORINS. Minimization of FWM effect in nonlinear optical fibre using variable channel spacing technique. *2016 Advances in Wireless and Optical Communications (RTUWO)* [online]. November 2016 [cit. 2021-04-12]. Available from: https://ieeexplore.ieee.org/document/7821844

[27] EL-HALAFAWY, Farag Z., Moustafa H. ALY and Maha A. ABD EL-BARY. Four-Wave Mixing Crosstalk in DWDM Optical fibre Systems. *Proceedings of the Twenty Third National Radio Science Conference (NRSC'2006)* [online]. March 2006 [cit. 2021-04-12]. Available from: https://ieeexplore.ieee.org/document/4275155

[28] SUGUMARAN, S, Lokesh SHARMA and Shilpa CHOUDHARY. Optimized FWM Parameters for FTTH Using DWDM Network. *2019 International Conference on Computational Intelligence and Knowledge Economy (ICCIKE)* [online]. December 2019 [cit. 2021-04-12]. Available from: https://ieeexplore.ieee.org/document/9004281

[29] HUSZANÍK, Tomáš, Ján TURÁN and Lúboš OVSENÍK. On Mitigation of Four-Wave Mixing in High Capacity Ultra-DWDM System. *2019 20th International Carpathian Control Conference (ICCC)* [online]. May 2019 [cit. 2021-04-12]. Available from: https://ieeexplore.ieee.org/document/8766021

[30] MANZOOR, Habib Ullah, Abaid Ullah SALFI, Tayyab MEHMOOD and Tareq MANZOOR. Reduction of Four Wave Mixing by employing circular polarizers in DWDM optical networks. *2015 12th International Bhurban Conference on Applied Sciences and Technology (IBCAST)* [online]. January 2015 [cit. 2021-04-12]. Available from: https://ieeexplore.ieee.org/document/7058574

[31] SUGUMARAN, S. and P. ARULMOZHIVARMAN. Effect of chromatic dispersion on four-wave mixing in WDM systems and its suppression. *2013 International Conference on Emerging Trends in VLSI, Embedded System, Nano Electronics and Telecommunication System (ICEVENT)* [online]. January 2013 [cit. 2021-04-12]. Available from: https://ieeexplore.ieee.org/document/6496567

[32] KAUR, Gurleen and Gurinder SINGH. Analysis to find the best Hybrid modulation technique for suppression of Four Wave Mixing. *2015 2nd International Conference on Recent Advances in Engineering and Computational Sciences (RAECS)* [online]. December 2015 [cit. 2021-04-12]. Available from: https://ieeexplore.ieee.org/document/7453294

[33] QAMAR, Farhan, Khawar ISLAM and Romana FARHAN. DWDM system analysis by varying different erbium doped fibre parameters. *2018 International Conference on Engineering and Emerging Technologies (ICEET)* [online]. February 2018 [cit. 2021-04-12]. Available from: https://ieeexplore.ieee.org/document/8338616

[34] KAUR, Inderpreet and Neena GUPTA. Optimization of fibre length for EDFA to enhance the channel capacity of DWDM system. *2012 International Symposium on Instrumentation and Measurement, Sensor Network and Automation (IMSNA)* [online]. August 2012 [cit. 2021-04-12]. Available from: https://ieeexplore.ieee.org/document/6324504

[35] ZAMAN, Mubashir ul, Shahid IQBAL and ISHA. Performance analysis of EDFA amplifier for DWDM system. *2014 International Conference on Computing for Sustainable Global Development (INDIACom)* [online]. March 2014 [cit. 2021-04-12]. Available from: https://ieeexplore.ieee.org/document/6828081

[36] PATNI, Amit and Durgesh KUMA. Simulation of gain flattened 32 channels EDFA-DWDM optical system. *2016 International Conference on Recent Advances and Innovations in Engineering (ICRAIE)* [online]. December 2016 [cit. 2021-04-12]. Available from: https://ieeexplore.ieee.org/document/7939600

[37] LAVRINOVICA, Ingrida and Jurgis PORINS. Noise Figure Analysis of EDFA with different pumping configurations in 40 Gbit/s 8 channel DWDM transmission system. *2015 Advances in Wireless and Optical Communications (RTUWO)* [online]. November 2015 [cit. 2021-04-12]. Available from: https://ieeexplore.ieee.org/document/7365714

[38] PUTRINA, Julija, Sergejs OLONKINS and Vjaceslavs BOBROVS. Investigation of EDFA positioning impact on the quality of the amplified signal in DWDM transmission systems. *2017 Electronics* [online]. June 2017 [cit. 2021-04-12]. Available from: https://ieeexplore.ieee.org/document/7995230

[39] AGUIAR, Douglas, Giorgio GRASSO, Aldo RIGHETTI and Fausto MELI. EDFA with continuous amplification of C and L bands for submarine applications. *2015 SBMO/IEEE MTT-S International Microwave and Optoelectronics Conference (IMOC)* [online]. November 2015 [cit. 2021-04-12]. Available from: https://ieeexplore.ieee.org/document/7369198

[40] AGALLIU, Rajdi and Michal LUCKI. System improvements in dense wavelength division multiplexing networks by using advanced optical modulation formats. *2015 17th International Conference on Transparent Optical Networks (ICTON)* [online]. July 2015 [cit. 2021-04-12]. Available from: https://ieeexplore.ieee.org/document/7193511

[41] WINZER, P.J. and R.J. ESSIAMBRE. Advanced Optical Modulation Formats. *Proceedings of the IEEE* [online].

June 2006, **94**(5), 952 - 985 [cit. 2021-04-12]. Available from: https://ieeexplore.ieee.org/document/1634536?arnumber=1634536

[42] ZHANG, Guodong, Pedro MELEDINA, Craig SKOLNICK and Gary ARMIENTO. Assessment of capacity upgrade using 40Gbps DPSK transmission in 10Gbps DWDM ROADM networks. *2011 Optical fibre Communication Conference and Exposition and the National fibre Optic Engineers Conference* [online]. March 2011 [cit. 2021-04-12]. Available from: https://ieeexplore.ieee.org/document/5875202

[43] EHRHARDT, A., D. BREUER, D. FRITZSCHE, S. VORBECK, et al. Field Trial to Upgrade an Existing 10 Gbit/s DWDM Link by 40 Gbit/s RZ-DQPSK Channels. *2007 9th International Conference on Transparent Optical Networks* [online]. July 2007 [cit. 2021-04-12]. Available from: https://ieeexplore.ieee.org/document/4296024

[44] YAO, Shuchang, Songnian FU, Hantao WANG and Ming TANG. Performance comparison for NRZ, RZ, and CSRZ modulation formats in RS-DBS Nyquist WDM system. *IEEE/OSA Journal of Optical Communications and Networking* [online]. April 2014, **6**(4), 355 - 361 [cit. 2021-04-12]. Available from: https://ieeexplore.ieee.org/document/6821325

[45] LATAL, Jan, Jan VITASEK, Petr KOUDELKA, Petr SISKA, et al. Simulation of modulation formats for optical access network based on WDM-PON. *2014 16th International Conference on Transparent Optical Networks (ICTON)* [online]. July 2014 [cit. 2021-04-12]. Available from: https://ieeexplore.ieee.org/document/6876473

[46] KURBATSKA, Inna, Sandis SPOLITIS, Vjaceslavs BOBROVS, et al. Performance comparison of modulation formats for 10 Gbit/s WDM-PON systems. *2016 Advances in Wireless and Optical Communications (RTUWO)* [online]. November 2016 [cit. 2021-04-12]. Available from: https://ieeexplore.ieee.org/document/7821854

[47] WANG, Liang, Marco FORZATI and Jonas MARTENSSON. Analysis of NRZ- and RZ-DQPSK for 112 Gb/s DWDM transmission. *2009 11th International Conference on Transparent Optical Networks* [online]. July 2009 [cit. 2021-04-12]. Available from: https://ieeexplore.ieee.org/document/5185006

[48] TAHER, Kazi Abu, Satya P. MAJUMDER and B. M. Azizur RAHMAN. Performance of different modulation formats in 40 Gb/s optical systems in the presence of polarization mode dispersion and nonlinear effects. *2014 International Conference on Electrical Engineering and Information and Communication Technology* [online]. April 2014 [cit. 2021-04-12]. Available from: https://ieeexplore.ieee.org/document/6919042

[49] PRIYEASH, B. and N. SUBHASHINI. Performance of Hybrid PON Architecture using On-Off Keying and Differential Quadrature Phase

Shift Keying. *2020 International Conference for Emerging Technology (INCET)* [online]. June 2020 [cit. 2021-04-12]. Available from: https://ieeexplore.ieee.org/document/9153976

[50] VAN DEN BORNE, D., S. L. JANSEN, E. GOTTWALD, et al. 1.6-b/s/Hz Spectrally Efficient Transmission Over 1700 km of SSMF Using 40 x 85.6-Gb/s POLMUX-RZ-DQPSK. *Journal of Lightwave Technology* [online]. March 2007, **25**(1), 222-232 [cit. 2021-04-12]. Available from: https://ieeexplore.ieee.org/document/4137619

[51] VAN DEN BORNE, D., S. L. JANSEN, G.D. KHOE, et al. A comparison between multi-level modulation formats: 21.4-Gbit/s RZ-DQPSK and POLMUX-RZ-DPSK. *2006 Optical fibre Communication Conference and the National fibre Optic Engineers Conference* [online]. March 2006 [cit. 2021-04-12]. Available from: https://ieeexplore.ieee.org/document/1636930

[52] SLEIFFER, V. A. J. M., M. S. ALFIAD, D. VAN DEN BORNE, et al. A comparison of 43-Gb/s POLMUX-RZ-DPSK and POLMUX-RZ-DQPSK modulation for long-haul transmission systems. *36th European Conference and Exhibition on Optical Communication* [online]. September 2010 [cit. 2021-04-12]. Available from: https://ieeexplore.ieee.org/document/5621432

[53] BAJPAI, Rochak, Sujata SENGAR and Shree Prakash SINGH. Comparison of performance of a mixed line rate optical WDM network using different modulations at 40Gbps. *2016 International Conference on Advances in Computing, Communication and Automation (ICACCA) (Spring)* [online]. April 2016 [cit. 2021-04-12]. Available from: https://ieeexplore.ieee.org/document/7578869

[54] CHANDRASEKHAR, S. and X. LIU. Impact of Channel Plan and Dispersion Map on Hybrid DWDM Transmission of 42.7-Gb/s DQPSK and 10.7-Gb/s OOK on 50-GHz Grid. *IEEE Photonics Technology Letters* [online]. October 2007, **19**(22), 1801 - 1803 [cit. 2021-04-12]. Available from: https://ieeexplore.ieee.org/document/4367519

[55] WUTH, T., M.W. CHBAT and V.F. KAMALOV. Multi-rate (100G/40G/10G) Transport Over Deployed Optical Networks. *OFC/NFOEC 2008 - 2008 Conference on Optical fibre Communication/National fibre Optic Engineers Conference* [online]. February 2008 [cit. 2021-04-12]. Available from: https://ieeexplore.ieee.org/document/4528299

[56] ALFIAD, Mohammad S., Maxim KUSCHNEROV and Torsten WUTH. 111-Gb/s Transmission Over 1040-km Field-Deployed fibre With 10G/40G Neighbors. *IEEE Photonics Technology Letters* [online]. February 2009, **21**(10), 615 - 617 [cit. 2021-04-12]. Available from: https://ieeexplore.ieee.org/document/4787123

[57] XIA, T.J., G. WELLBROCK and D. PETERSON. Multi-rate (111-Gb/s, 2x43-Gb/s, and 8x10.7-Gb/s) transmission at 50-GHz channel spacing over 1040-km field-deployed fibre. *2008 34th European Conference on Optical Communication* [online]. September 2008 [cit. 2021-04-12]. Available from: https://ieeexplore.ieee.org/document/4729413

[58] *Optsim: User Guide* [online]. USA, 2008 [cit. 2020-11-17]. RSoft Design Group, Inc.

[59] Q-factor test equipment to estimate the transmission performance of optical channels: ITU-T recommendation O.201. *ITU* [online]. Switzerland, Geneva, 2003 [cit. 2021-04-12]. Available from: https://www.itu.int/rec/T-REC-O.201-200307-I/en

[60] What is Q-factor and what is its importance? *MapYourTech.com*[online]. [cit. 2021-01-15]. Available from: https://mapyourtech.com/entries/general/what-is-q-factor-and-what-is-its-importance-

[61] ITU-T G-series Recommendations – Supplement 39: Optical system design and engineering considerations. *ITU* [online]. Switzerland, Geneva, 2016 [cit. 2021-02-26]. Available from: https://www.itu.int/rec/T-REC-G.Sup39-201602-I/en

[62] ITU-T SERIES G: TRANSMISSION SYSTEMS AND MEDIA, DIGITAL SYSTEMS AND NETWORKS: Higher speed passive optical networks – Requirements. *ITU* [online]. Switzerland, Geneva, 2020 [cit. 2021-03-13]. Available from: https://www.itu.int/rec/T-REC-G.9804.1/en

[63] LI, Qiwang, Min ZHANG and Zhuo LIU. Investigation of 20Gb/s WDM-PON transmission over 40-km employing 16QAM signal with blind equalization. *2013 8th International Conference on Communications and Networking in China (CHINACOM)* [online]. August 2013 [cit. 2021-04-12]. Available from: https://ieeexplore.ieee.org/document/6694693

[64] *Optsim: Application Notes and Examples* [online]. RSoft Design Group [cit. 2021-04-21].

[65] *Optsim: Sample Mode - Models Reference* [online]. RSoft Design Group [cit. 2021-04-21].